

AD-A158 101

1

CBR DESIGN OF FLEXIBLE AIRFIELD PAVEMENTS
WITH CASE STUDY

By

THOMAS M. DESTAFNEY

A REPORT PRESENTED TO THE GRADUATE COMMITTEE
OF THE DEPARTMENT OF CIVIL ENGINEERING IN
PARTIAL FULFILLMENT OF THE REQUIREMENTS
FOR THE DEGREE OF MASTER OF ENGINEERING

UNIVERSITY OF FLORIDA

Spring 1985

DTIC FILE COPY

This document has been approved
for public release and sale; its
distribution is unlimited.

8 DTIC
SELECTED
AUG 16 1985
S D

85

8 9

108

AD NUMBER	DATE	DESTAFNEY, T.	DTIC ACCESSION NOTICE
1. REPORT IDENTIFYING INFORMATION		REQUESTER:	
<p>A. ORIGINATING AGENCY NAVAL POSTGRADUATE SCHOOL, MONTEREY, CA 93943. Put your mailing address on reverse of form.</p> <p>B. REPORT TITLE AND/OR NUMBER CBR DESIGN OF FLEXIBLE AIRFIELD PAVEMENTS WITH CASE</p> <p>C. MONITOR REPORT NUMBER STUDY</p> <p>by: Thomas M. Destafney. Thesis. U-Florida</p> <p>D. PREPARED UNDER CONTRACT NUMBER N66314-72-A-3029</p> <p>Spring 1985 DTIC:</p>			
2. DISTRIBUTION STATEMENT		<p>Approved for public release: distribution unlimited</p>	

DTIC FORM 50
DEC 80

PREVIOUS EDITIONS ARE OBSOLETE

CBR DESIGN OF FLEXIBLE AIRFIELD PAVEMENTS
WITH CASE STUDY

By

THOMAS M. DESTAFNEY

A REPORT PRESENTED TO THE GRADUATE COMMITTEE
OF THE DEPARTMENT OF CIVIL ENGINEERING IN
PARTIAL FULFILLMENT OF THE REQUIREMENTS
FOR THE DEGREE OF MASTER OF ENGINEERING

UNIVERSITY OF FLORIDA

Spring 1985

This document has been approved
for public release and sale; its
distribution is unlimited.



Accession For	
NTIS GRAS	<input checked="" type="checkbox"/>
DTIC TAB	<input type="checkbox"/>
Unannounced	<input type="checkbox"/>
Justification	
per Form 50 on file	
By _____	
Distribution/	
Availability Codes	
Avail and/or	
Dist	Special
A-1	

To Camille, Neal and Cara

TABLE OF CONTENTS

	Page
CHAPTER ONE - INTRODUCTION -----	1
1.1 Purpose -----	1
1.2 History and Trends in Design -----	1
1.3 Airfield Pavement Structures -----	3
1.4 Fundamental Flexible Pavement Theory -----	5
CHAPTER TWO - DYNAMIC LOADS AND AIRCRAFT WANDER -----	9
2.1 Dynamic Effects -----	9
2.2 Aircraft Wander -----	10
2.2.1 Lateral Traffic Distribution -----	11
2.2.2 Effects of Aircraft Wander on Pavements -----	14
2.2.2.1 Traffic Areas -----	16
CHAPTER THREE - PRELIMINARY DATA ESSENTIAL FOR DESIGN -----	17
3.1 Introduction -----	17
3.2 Subgrade Investigation and Evaluation -----	17
3.2.1 CBR Test Procedure -----	18
3.3 Landing Gear Configurations and Tire Pressures -----	21
3.4 Aircraft Loads and Repetitions -----	23
CHAPTER FOUR - CORPS OF ENGINEERS CBR DESIGN AND PROCEDURE ---	27
4.1 History and Development -----	27
4.2 Adaptation of CBR Method to Airfield Pavements -----	27
4.3 CBR Thickness Design Procedure -----	29
4.3.1 Subgrade and Subbase Design CBF Selection ---	31
4.3.2 Design Aircraft Selection and Traffic Forecasting -----	33
4.3.3 Minimum Pavement Thickness -----	33
4.3.4 Determination of the ESWL -----	34
4.3.5 CBR Design Curve Development -----	41
4.4 Design for Protection Against Frost -----	45

CHAPTER FIVE - CASE STUDY: PALAU AIRFIELD -----	55
5.1 Introduction -----	55
5.1.1 Palau Climate and Geology -----	57
5.2 Palau Airfield Design -----	58
5.2.1 Existing Airfield and Design Parameters ---	58
5.2.2 New Airfield Design and Construction Criteria -----	60
5.2.3 Palau Airfield, FAA Design -----	62
5.2.4 Performance of the Palau Airfield -----	62
5.3 Palau Airfield CBR Design -----	65
5.3.1 Design Criteria -----	65
5.3.1.1 Subgrade CBR Design -----	65
5.3.1.2 Subbase and Base Design CBR Values --	66
5.3.1.3 Minimum Pavement Thickness -----	66
5.3.1.4 Design Aircraft -----	67
5.3.1.5 Forecasted Annual Aircraft Operations	69
5.3.2 ESWL Calculations -----	71
5.3.3 CBR Design Curve Development -----	76
5.3.4 Pavement Thickness Determination -----	77
5.4 Comparison of Design Results -----	82
CHAPTER SIX - CONCLUSION -----	85
6.1 Conclusion -----	85
REFERENCES -----	87

CHAPTER ONE

INTRODUCTION

1.1 Purpose

It is the purpose of this paper to state the fundamentals involved in the design of flexible airfield pavements utilizing the U.S. Army Corps of Engineers (COE) CBR (California Bearing Ratio) design method. This paper will also discuss concepts that are considered to be prerequisites to any discussion of the subject, including basic pavement theory, aircraft loading effects, subgrade strength, and aircraft characteristics related to design. The CBR method of design will be outlined, and an actual design performed in order to more clearly illustrate this method of designing flexible airfield pavements.

1.2 History and Trends in Design

Airport design and construction has become a modern day civil engineering skill that encompasses all major aspects of the profession. The rapid development of aircraft size and landing gear wheel configurations over the past 40 to 50 years has had a profound affect on the design and construction of one phase in particular, that of airfield pavements.

Prior to World War II, airfield pavements, both flexible and rigid, were designed and constructed based on standard, "canned" designs and cross-sections. During the war, increased bombing and transport

requirements of the military created a need for larger and therefore heavier aircraft that had larger payload capacities. As Figure 1-1 shows, the years 1950-1980 saw aircraft grow larger still, as civilian airlines found it more economical to transport increasing numbers of passengers in larger and heavier aircraft (6:65). Not only have aircraft weights increased, but their frequency of operation has greatly increased. Worse yet, aircraft have historically increased in weight throughout the evolution of their useful lives, and usually without a change in the number or spacing of its wheels (13:640). This growth in aircraft weight coupled with the continued increase in the number of operations has led to the development of several pavement design methods, most of which were derived from existing highway design methods (1:39).

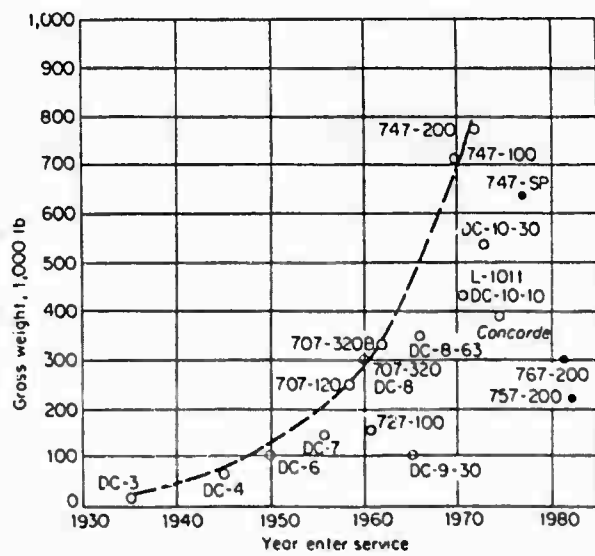


Figure 1-1. Trends in the Weight of Transport Aircraft

Over the years there has been a steady trend towards expanding the concepts of pavement design. Initially, the only considerations were subgrade strength, load, and pavement thickness. Concepts have been expanded to include climactic effects (i.e. frost action), material quality, tire pressures, load repetition, landing gear wheel configuration (multiple wheels), skid resistance, and roughness. The jumbo jet has placed a new emphasis on the need for a better understanding of a pavement subjected to an aircraft loading. The Boeing 747 and Lockheed C5A Galaxy, for example, give civil engineers good reason to be concerned. They are both high use, high weight (over 750,000 lbs.) aircraft that are partially responsible for many of the new concepts in design listed above.

1.3 Airfield Pavement Structures

A pavement or pavement structure can be defined as a structure consisting of one or more layers of processed materials (6:420). A pavement that is composed of portland cement concrete is referred to as rigid, whereas one consisting of a mixture of aggregate and bituminous material is referred to as a flexible pavement. This paper will discuss the design of flexible airfield pavements only. It should be pointed out that throughout this paper the term "design" will refer only to the determination of the thickness of the pavement and its components.

The principal functions of a flexible airfield pavement are to provide air traffic with a smooth, safe operating surface which can withstand any applied load or environmental influence for some prescribed period of operation (6:420). The thickness of each layer must be sufficient to insure that any applied loads will not cause a failure in it or in any of the underlying layers. As Figure 1-2 shows, a typical

pavement is composed of a surface course, base course, and subbase course, all of which rest on a compacted subgrade. The surface course, or wearing course as it is sometimes called, is composed of rock aggregate and asphalt and ranges in thickness from three or four inches to thicknesses of 12 inches or more. The wearing course is intended to prevent the penetration of water to the base layer, provide a smooth riding, well bonded surface that is free of loose particles and debris, and to provide resistance to any shear stresses due to aircraft wheel loads. The pavement should also be resistant to fuel and other solvents in locations where operations increase the likelihood of a spill.

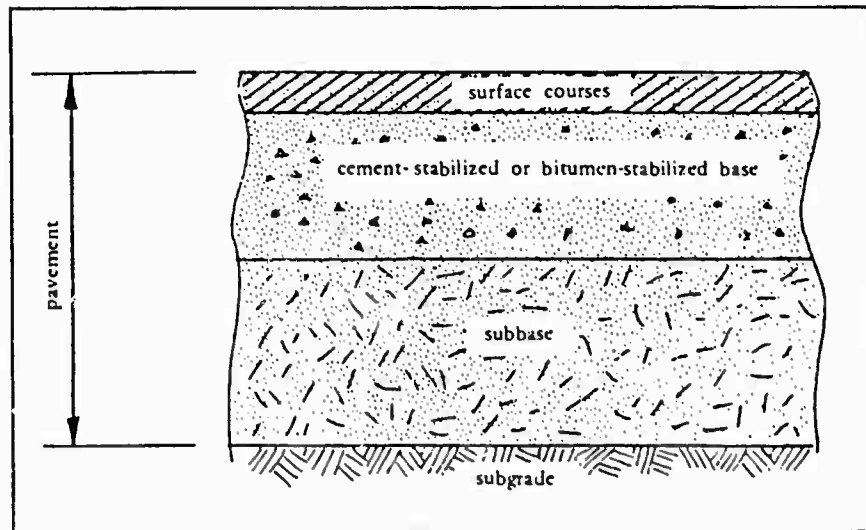


Figure 1-2. Typical Flexible Pavement Components

The base course is intended to distribute wheel loads to the sub-base and subgrade. It must be capable of protecting the subgrade from failure, withstanding the stresses within itself, resisting any vertical stresses tending to cause consolidation or deformation of the wearing course, and resisting any change in volume due to a fluctuation in moisture content.

The subbase layer must simply be capable of protecting the subgrade by withstanding the stresses existing at its own depth. This optional layer is used in areas where frost action is severe or in locations where the subgrade is extremely weak.

The subgrade is exposed to lower stresses than any of the overlying layers, as stress decreases with depth. This foundation layer must have the strength to withstand the stresses existing at the subgrade depth.

A flexible airfield pavement may also be classified as a full-depth asphalt pavement, which is a flexible pavement that has all courses above the improved or compacted subgrade composed of asphalt mixtures. The design of typical airfield flexible pavements will be further discussed in Chapters 4 and 5.

1.4 Fundamental Flexible Pavement Theory

The CBR method of flexible pavement design was developed by the Corps of Engineers by studying the effects of uniform circular loads acting on a homogeneous, isotropic, and elastic half-space. These three conditions are the assumptions made by the nineteenth-century French mathematician, Boussinesq, as he studied the distribution of stress, strain, and deflection in a media beneath a point load on the surface (8:163).

Vertical stresses beneath a point load have a bell shaped distribution. The maximum stresses occur directly beneath the point of application. The stresses are maximum near the surface and theoretically decrease to zero at an infinite depth.

For the study of flexible pavements, the surface loading is not a point load, but is distributed over an elliptical area, although assumed to be circular for design purposes. The vertical stresses at the tire-pavement interface are equivalent to the tire pressure and the variation in vertical stress with depth follows the same distribution as for a point load.

Figure 1-3 shows a circular load of radius r and pressure p . The vertical stress, σ_v , at any point beneath the load is dependent on the vertical distance, z , beneath the surface and the radial distance or offset, r , from the point or center of load application.

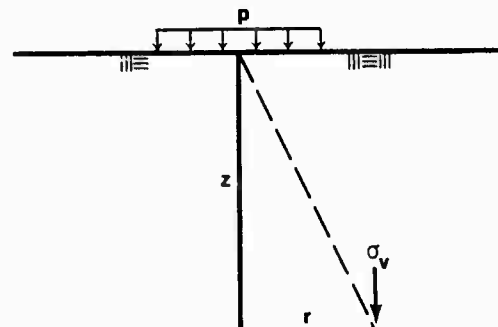


Figure 1-3. Vertical Stress Under Uniform Circular Load

1.4.1 Subgrade Deflection

The amount of subgrade deflection of a flexible pavement is an important design concept. The percentage of the surface deflection contributed by the deflection of the subgrade varies between 70 and 95 percent. It can therefore be assumed that most of the deflection, which is the integration of vertical strain with depth, is due to the elastic compression of the subgrade layer (14:73).

Generally, for analysis of flexible pavements, it is assumed that all pavement components above the subgrade do not contribute to the total surface deflection. The total surface deflection is equal to the deflection within the subgrade layer.

The COE analysis assumes that the pavement and subgrade together are considered to behave as a homogeneous, isotropic, elastic, semi-infinite medium. For tire applied loadings, subgrade deflections may be calculated through the following equation:

$$\Delta = \frac{paF}{E} \quad (1.1)$$

where

Δ = vertical deflection, in.

p = tire contact pressure, psi

a = radius of tire contact area, in.

E = modulus of elasticity, psi

F = deflection factor, a function of depth and
radial offset from load centerline

The modulus of elasticity E and Poisson's ratio are both important parameters in the study of deflections under loads. The modulus of

elasticity is defined as the stress to strain ratio and in equation 1.1 is assumed to be constant. The greater the modulus of elasticity, the higher the resistance to elastic deformation. The modulus of elasticity is assumed to be constant throughout the pavement and equal to the modulus of the subgrade material (12:29).

Poisson's ratio is defined as the ratio of the transverse strain to longitudinal strain, which expresses a material's ability to increase its transverse dimensions under a compressive load or decrease its transverse dimensions under the effects of a longitudinal, tensile load. The COE CBR design theory is based on a Constant Poisson's ratio of 0.5.

CHAPTER TWO

DYNAMIC LOADS AND AIRCRAFT WANDER

2.1 Dynamic Effects

The dynamic responses of aircraft, specifically acceleration and deceleration forces, can be considerably more severe than those for even the largest of trucks. An aircraft undercarriage assembly may transmit a load greater than the static weight to the pavement due to these dynamic effects.

This may be best demonstrated by considering the following three critical conditions. First, consider the point of impact on the runway during an aircraft landing. As the aircraft lands, its weight is carried aerodynamically and the resulting pavement loading is, to a large degree, due to the downward velocity component (sink rate) of the aircraft. The degree of this downward velocity component can range from a high value due to a poorly executed landing to a low value due to a well executed landing. Other than surface scuffing and scratching, there is no evidence that this area of the pavement typically suffers structural overload due to this action (1:9).

The second condition considers the rotation of an aircraft during takeoff. As the aircraft gains speed and begins rotation, the nose gear is lifted off the ground, thereby transferring all weight to the main gear assembly. This weight is increased by the increasing aerodynamic force on the elevator. This condition, known as the "spike effect", has never been observed to cause pavement failure (1:9-10).

The third condition is the most critical with regard to flexible pavements and has been documented as having accelerated pavement failure. It involves the centrifugal effects of taxiing on turn-offs and turn-ons to runways. In turning, particularly on hot days, an aircraft can create a large shear force that tends to push the underlying asphalt outside the turn, possibly resulting in displacement of the pavement (1:10).

Despite the documented failures due to centrifugal effects, it is a lack of large scale evidence of all three of the above conditions that has led to the conclusion that these dynamic effects are not more critical from a design standpoint than the conditions encountered for a static or taxiing aircraft at maximum gross takeoff weight (14:447). Therefore, flexible airfield pavements are designed based on the design aircraft's maximum gross takeoff weight.

2.2 Aircraft Wander

An aircraft pass may be defined as one passage of a single aircraft at the critical design location. This critical design location is generally a taxiway, as this is where most damage to the pavement is anticipated. Airfield pavements are normally designed for a given number of passes of a design aircraft. The number of times a pavement is subjected to the design aircraft's maximum load determines the pavement's ultimate life span. An aircraft pass is not to be confused with an application of the maximum stress, or a coverage. The relationship and difference between the terms pass and coverage and the effects of aircraft wander on airfield pavement design will be discussed in this section.

2.2.1 Lateral Traffic Distribution

Most airfield runway and taxiway centerlines are marked to aid pilots in landing, taking off, and taxiing. This convenience has resulted in more channelized aircraft traffic, with the highest concentration being in the centerline area of the runway (12:8). Despite this, aircraft are much more widely distributed laterally than highway vehicles. From a theoretical standpoint, there is an equal chance of an aircraft deviating to the right or left of the centerline. Because airfields are usually designed to withstand a large number of aircraft passes, the traffic may be considered to be normally distributed and represented by a normal curve. Figure 2-1 presents actual distribution curves derived from field observations at three U.S. Air Force airfields. Note how both actual observed curves follow the theoretical normal distribution curve.

Aircraft wander may be defined as the width over which the centerline of airfield traffic is distributed 75 percent of the time. A wander width or design traffic width of 70 inches is applied to taxiways and the first 1,000 feet at each runway end, while a wander width of 140 inches is used for runway interiors. These values are based on field observations (12:11).

An aircraft coverage is defined as when each point of the pavement within the design traffic width receives one application of load (14:158). Each aircraft pass, or operation, applies only a partial coverage each time it taxies, takes off, or lands. The number of coverages per pass or operation is dependent on the tire width, number of tires per gear, the design traffic width, and the percent traffic in the design lane (75 percent).

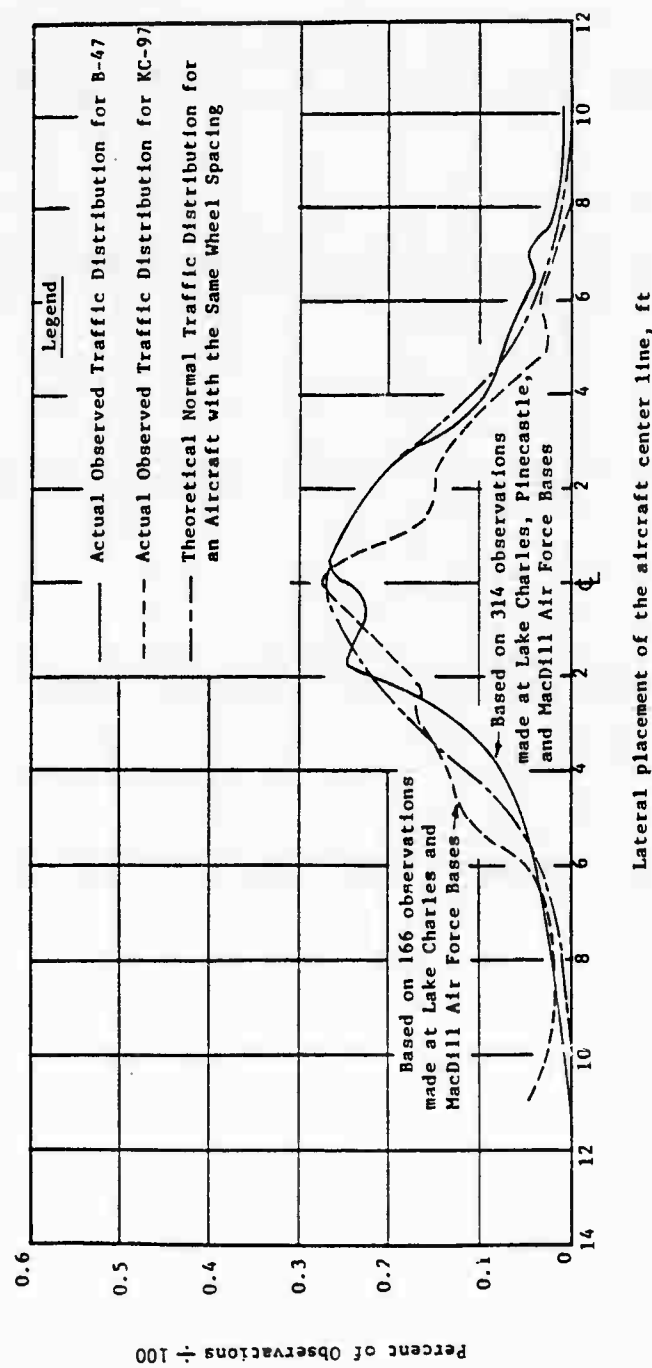


Figure 2-1. Distribution of Aircraft Traffic About Centerline

This concept may be best demonstrated by considering a one tire aircraft and its movements on an airfield pavement. Figure 2-2 shows the normal distribution of traffic about a taxiway centerline with a wander width of 70 inches and tire width W_t . As defined, 75 percent of all aircraft passes fall within the shaded regions of the normal curve, between lines drawn at 35 inches right and 35 inches left of the taxiway centerline. Assume that the normal distribution curve shown in Figure 2-2 is divided transversely into strips, with each strip being W_t inches wide. Each time the aircraft tire passes over the center strip, a coverage is being applied to that strip. For design purposes, the number of coverages applied to the pavement is defined as the number of coverages applied to that strip where the maximum accumulation occurs (12:12).

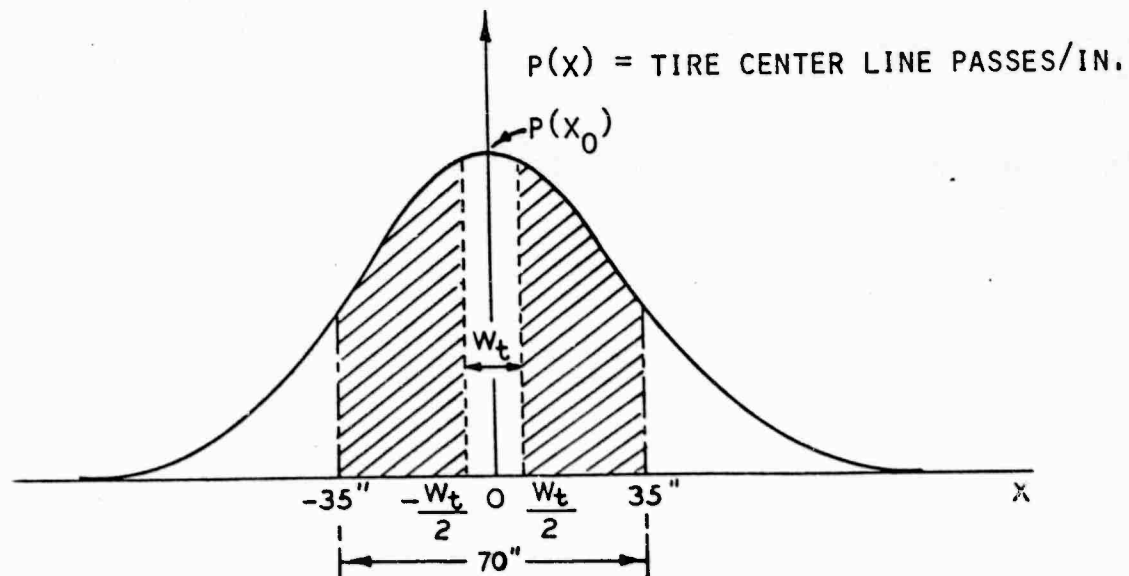


Figure 2-2. Normal Distribution of Aircraft Traffic About Centerline

Now, assume that aircraft traffic is applied to the taxiway so that in 100 aircraft passes, the aircraft tire runs over the center strip of W_t inches in width 20 times. In this particular example, 20 coverages have been applied and the coverage to pass ratio is equal to $20/100 = 0.20$, or the pass to coverage ratio is equal to $100/20 = 5.0$.

By using the basic analysis just presented, the Corps of Engineers has derived equations that can be used to calculate the number of coverages per pass for any aircraft. The conversion from passes to coverages used to be quite important to the designer, as the number of coverages was used to determine load repetition factors, which are thickness adjustment factors that are based on the number of passes or operations and the number of gear tires in each main assembly. However, further analysis by the COE has simplified the process by deleting the requirement to convert passes to coverages for load repetition factor determination. Curves have been generated for determining the factor based on the number of aircraft passes and the number of main gear tires per assembly. Despite this simplification, it is important that the designer understand the basic concepts of aircraft passes versus coverages.

2.2.2 Effects of Aircraft Wander on Pavements

As previously stated, aircraft have more lateral space available for transverse wander than do vehicles on highways. Highway vehicles, for example, have an average transverse standard deviation of about one foot. Aircraft on taxiways that have painted centerlines have a standard deviation between 2.0 and 3.5 feet. During take-off, aircraft standard deviations vary between 7.5 and 15 feet while for landing, the standard

deviation ranges from 13 to 20 feet (14:155). Due to the highly channelized effect of highway traffic, each vehicle pass or movement is considered to be one stress repetition or coverage. This is not true for runways and taxiways due to the relative lack of channelized conditions.

Figure 2-3 shows the effects of the standard deviation of aircraft wander on pavement damage. The 3.5 feet standard deviation curve is representative of taxiway travel conditions. Because the lower standard deviation represents more channelized travel, the peak pavement damage occurs at the center of the main gears. Note that as the standard deviation increases, the peak damage moves towards the pavement centerline. The results of these principles are that taxiways tend to have higher failure rates near the main gear locations, while runways develop more distress at their centerlines. This theory has been proven accurate by field observations made at various airports (14:155-156).

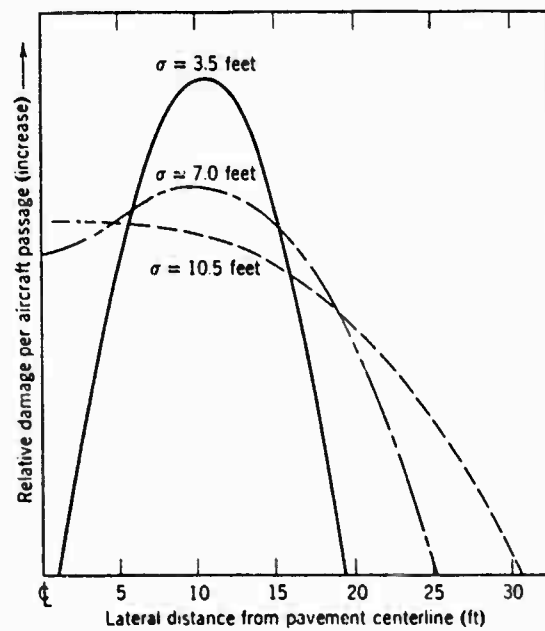


Figure 2-3. Effect of Standard Deviation of Aircraft Wander on Pavement Damage

2.2.2.1 Traffic Areas

Because relatively channelized traffic occurs on taxiways and runway ends, construction costs may be reduced by allowing a thinner pavement at the runway edges and other low-use areas. In order to take advantage of the variability of traffic volume over different areas of airfield pavements, the COE has categorized these areas into zones of anticipated distress, or traffic areas (14:160).

Type A traffic areas are those that will be subjected to the highest concentration of maximum loaded aircraft. These include primary taxiways, aprons, and the first 500 feet of each runway end. These areas are designed for 25,000 coverages of heavy, multiple-wheel aircraft.

Type B traffic areas are those areas exposed to a normal distribution of maximum loaded aircraft. These include the second 500 feet of each runway end, parking, and maintenance area pavements. They are designed for 5000 coverages of the design aircraft.

Type C traffic areas are those exposed to partial aircraft loads and includes the runway interior, secondary taxiways, and calibration hardstands. These areas are designed for 5000 coverages of the design aircraft at 75 percent of gross load.

CHAPTER THREE

PRELIMINARY DATA ESSENTIAL FOR DESIGN

3.1 Introduction

An airfield pavement is intended to protect the subgrade from shear failure due to aircraft loads applied at the surface. These loads are distributed by the tires to an acceptable level that will not exceed the strength of any pavement layer or the subgrade. Therefore, subgrade strength, design aircraft wheel configuration and tire pressures, and the magnitude and number of load repetitions are all data that is essential to flexible pavement design.

3.2 Subgrade Investigation and Evaluation

An accurate and thorough investigation of the supporting subgrade material is essential to the proper design of a flexible pavement. The greater the strength of the subgrade, the lower the required thickness of the pavement intended to protect it will be. Desirable subgrade characteristics include strength, good drainage, ease and permanency of compaction, and permanency of strength (14:328).

The subgrade investigation usually consists of a soil survey that will reveal the arrangement of the different soil layers in relation to the subgrade, the sampling and testing of soil from each layer to ascertain its physical properties with respect to in-place density and subgrade support, and a survey that will reveal the availability and suitability of local construction materials that will be used in the

construction of the pavement. Soil borings are generally used to accomplish the surveys and sampling which can be used to show the soil or rock profile and the lateral extent of each layer. Properties derived from field and lab tests include soil type, sieve analysis, Atterberg limits, moisture-density relationships, permeability, organic content, strength, and CBR. Table 3.1 contains general criteria for the spacing and depth of soil borings for airfield soil investigations (11:2-2).

Compaction requirements for airfield pavement subgrades are generally more strict than those intended for highways. Compaction of the subgrade to sufficient densities and sufficient depths is particularly important in areas of concentrated traffic on airfield runways, taxiways, and aprons. Standard test methods for subgrades, subbases, and base courses are given in Table 3-2 (10:4-6).

3.2.1 CBR Test Procedure

The CBR test is a penetration test and is expressed as a percentage of the penetration resistance to that of a standard value for crushed stone. The test consists of compacting about ten pounds of soil in a six inch diameter mold, immersing it in water for four days with a surcharge applied, and then penetrating the soaked sample with a two inch diameter piston at a specified loading rate. The soil's resistance to penetration, expressed as a percentage of that for a standard crushed stone, is the CBR design value. Therefore, a CBR of 50 means that the stress required to penetrate the sample 0.1 inch is only half of that required for the piston to penetrate that same distance in the standard crushed stone. The stress required to penetrate the standard stone to 0.1 inch is 1,000 psi.

**Table 3-1. Minimum Requirements for Spacing and Depth of
Exploratory Borings**

Item	Spacing Requirements
Runways and taxiways <200 feet wide	200 feet on center longitudinally, on alternating sides of the centerline
Runways >200 feet wide	three borings every 200 feet longitudinally, one boring on the centerline and one boring on each side of the centerline near the edges
Parking aprons and pads	one boring per 10,000-sq-ft area
Item	Depth Requirements
Cut areas	to a minimum of 10 feet below finished grade
Shallow fill (areas where not more than 6 feet of fill will be placed)	to a minimum of 10 feet below existing ground surface
High fill areas	to 50 feet below existing ground surface or to rock

Table 3-2. Standard Test Methods for Subgrades,
Subbases, and Base Courses

Test	Test Standard			Use		
	ASTM	AASHTO	MIL-STD-621 test method	Subgrade	Subbase	Base
Unit weight of aggregate.....	C29	T19				
Abbrasion of coarse aggregate by Los Angeles machine.....	C131	T96				
Specific gravity and absorption:						
Fine aggregate.....	C128	T84				
Coarse aggregate.....	C127	T85				
Sampling materials.....	D75	T2				
Compaction	D1557	T180	100 (CE55)			
In-Place density.....	D1556	T147				
In-Place moisture:						
Liquid limit	D423	T89	103			
Plastic limit	D424	T90	103			
Grain size analysis	C117					
Mechanical analysis	C475	T88				
Amount finer than						
No. 200 sieve.....	C136	T27				
Specific gravity	D1140	T11				
CBR test on compacted samples	C117					
CBR test undisturbed samples	D854	T100				
Field CBR test	D1883		101			
				101		
					101	

3.3 Landing Gear Configurations and Tire Pressures

As discussed in Chapter One, the last three decades have seen a very significant increase in aircraft size and weight. In order to more evenly distribute these loads on the pavement, aircraft have been modified by increasing the number of wheels supporting them. Figure 3-1 shows the effects of dual wheels on stresses for a constant tire pressure (14:77). In the figure, all tire pressures are 100 psi. As the figure shows, surface stresses are not affected by wheel configurations and are equal to the tire pressure. However, dual wheels result in increased stresses at greater depths due to an overlapping of pressure bulbs.

The vertical stress at a point due to a load acting on a pavement surface depends on both the applied pressure and the magnitude of the load. Figure 3-2 shows the effects of tire pressures on stress variation with depth (14:76). As the figure shows, a higher tire pressure creates higher vertical stresses in the upper layers of the pavement. Note that for the two 80 kip loadings, the vertical stresses are about equal at a depth of about 30-35 inches. Therefore, high tire pressures require the use of stronger materials in the upper layers of the pavement while not significantly affecting the pavement's total depth. For a constant tire pressure, an increase in load increases the vertical stress at any depth.

The load distribution between the nose gear and the main gears is dependent on the aircraft type and the location of the center of gravity. For airfield pavement design purposes, it is usually assumed that five percent of the aircraft gross weight is acting on the nose gear, with the remaining 95 percent supported by the main gears. It is also assumed that each tire on a main gear assembly supports a proportional amount of the weight acting on the assembly.

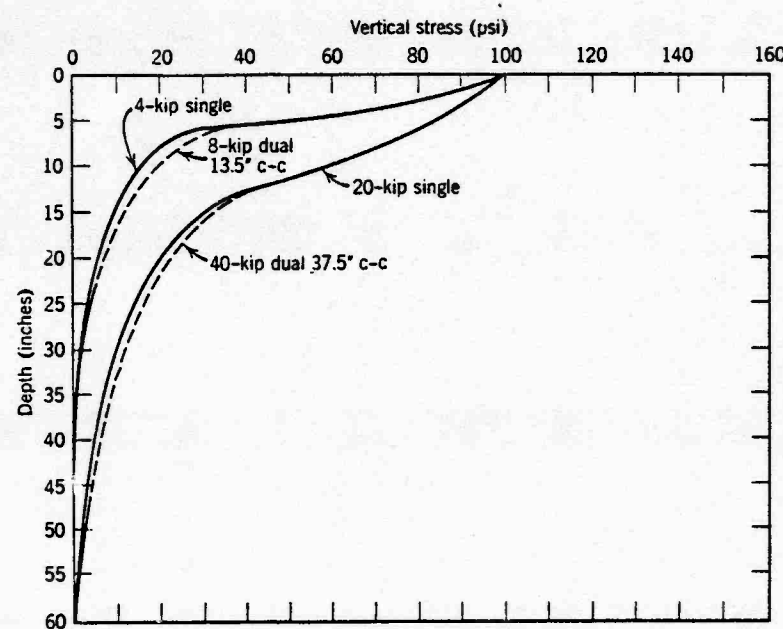


Figure 3-1. Effects of Dual Wheels on Vertical Stress

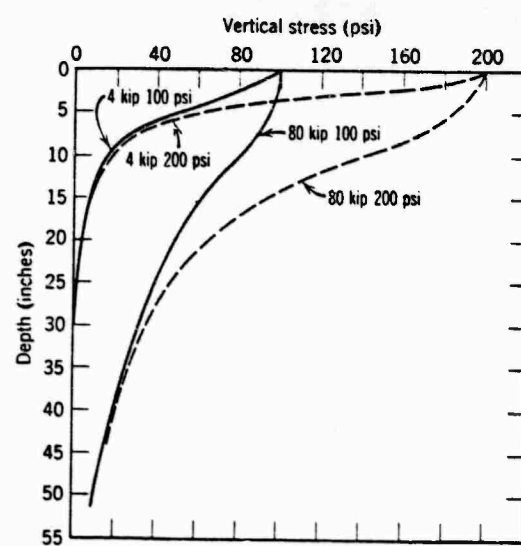


Figure 3-2. Effects of Tire Pressures on Stress Variation With Depth

The pavement designer needs to be intimately familiar with the effects of tire pressure and wheel configuration on a pavement. Table 3-3 shows the main landing gear configurations and tire pressures for some of the more common civilian aircraft in use today (6:63).

3.4 Aircraft Loads and Repetitions

Without question, an aircraft will inflict the most wear on a pavement when it is loaded to its maximum gross weight. Therefore, the design aircraft's maximum gross weight is one of the major parameters for flexible airfield pavement design.

Another important parameter related to aircraft weight is the number of loading cycles, or repetitions, that the pavement will be exposed to over its intended life.

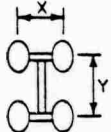
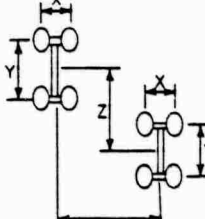
The design thickness, t , of a pavement may be expressed as

$$t = \alpha_i T \quad (3.1)$$

where T is the standard thickness for a particular aircraft and α_i is a load repetition factor that adjusts the pavement thickness. Experiments conducted at the U.S. Army Corps of Engineers Waterways Experiment Station have determined that the load repetition factor is dependent on the number of wheels in each main landing gear assembly and the estimated number of aircraft passes that the pavement will be subjected to (12:24). Therefore, for design purposes, a standard design thickness will be determined for the design aircraft and will be adjusted by the load repetition factor to account for the number of aircraft passes anticipated over the pavement's intended life. Figure 3-3 shows the load repetition factor versus passes curves for various landing gear

configurations. The application of these curves will be demonstrated in Chapter Five.

Table 3-3. Main Landing Gear Configurations and Tire Pressures for Common Aircraft

Main landing gear configuration	Aircraft	Dimensions, in				Typical inflation pressures, psi
		X	Y	Z	U	
	DC-9-80	28.1				170
	B-737	30.5				148
	B-727	34.0				168
	DC-8-61	30.0	55.0			188
	DC-8-62	32.0	55.0			187
	DC-8-63	32.0	55.0			196
	DC-10-10	54.0	64.0			173
	B-720B	32.0	49.0			145
	B-707-120B	34.0	56.0			170
	B-707-320B	34.6	56.0			180
	B-757	34.0	45.0			161
	B-767	45.0	56.0			183
	Concorde	26.4	65.7			184
	L-1011-500	52.0	70.0			184
	A-300B	35.0	55.0			168
	B-747A	44.0	58.0	121.2	142.0	204
	B-747B, C, F	44.0	58.0	121.2	142.0	185
	DC-10-30	54.0	64.0	30.0	216.0	157*
	DC-10-40	54.0	64.0	30.0	216.0	165'
				375		

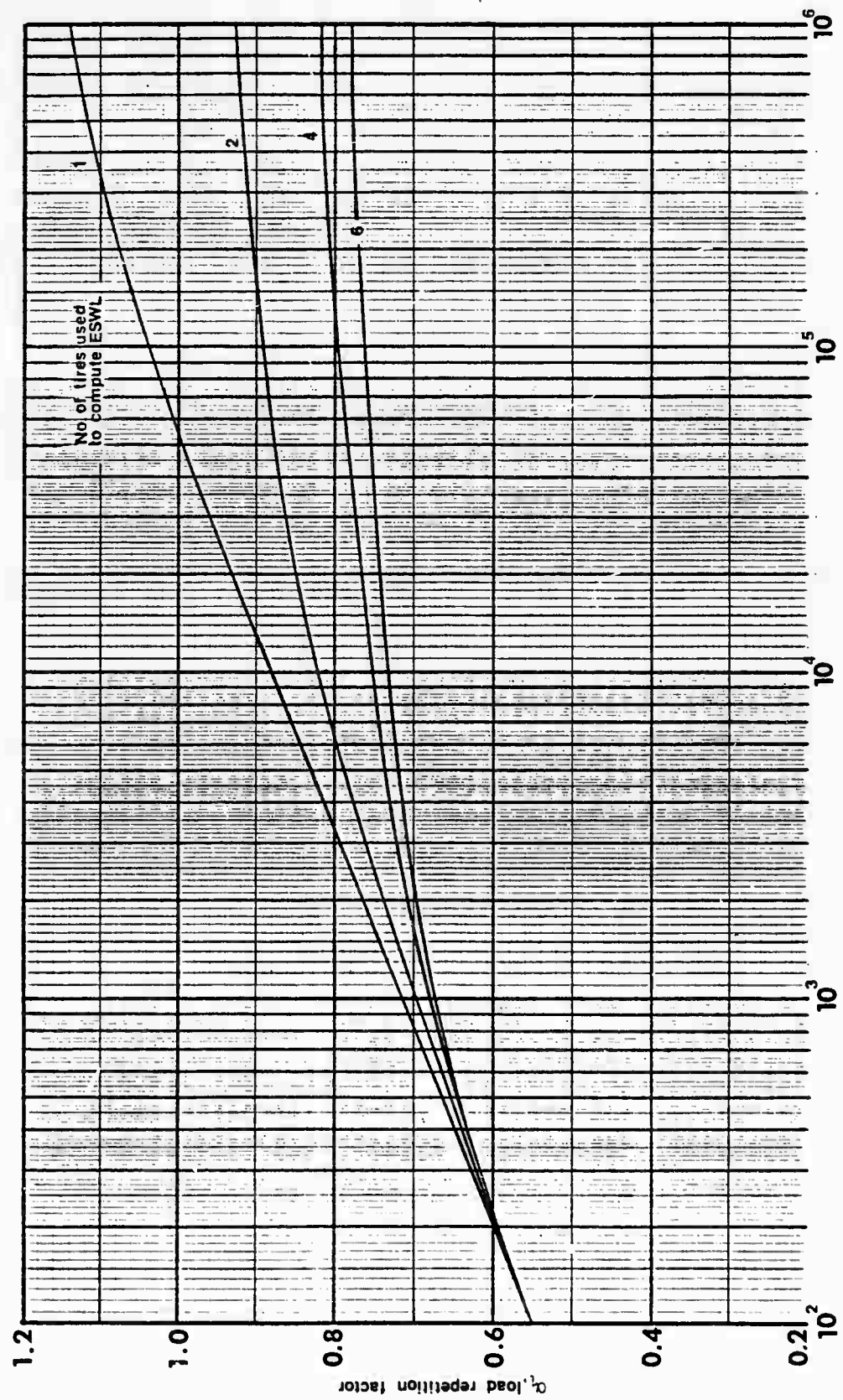


Figure 3-3. Composite Plot of Load Repetition Factors Versus Passes

CHAPTER FOUR

CORPS OF ENGINEERS CBR DESIGN AND PROCEDURE

4.1 History and Development

The California Division of Highways developed the CBR method of design in 1928. The outbreak of World War II required that an immediate decision be made by the U.S. Army concerning the choice of a design method, as there were no methods dedicated to the design of flexible airfield pavements. Obviously, the COE did not have the time required to develop a completely new method of design. Therefore, it was decided that a review of all existing flexible highway design methods would be made. The method that appeared the most adaptable to airfield use would be adopted and modified. After investigating all available methods for several months, the COE chose the CBR method because of its procedural simplicity, satisfactory performance, and ease in adapting it to airfield design (6:423).

4.2 Adaptation of CBR Method to Airfield Pavements

Between the years of 1928 and 1940, the California Highway Department (CHD) studied the adequacy of flexible pavements. From their observations, they developed the curves shown in Figure 4-1. Curve A was derived from pavements subjected to normally encountered highway conditions and curve B from light traffic conditions.

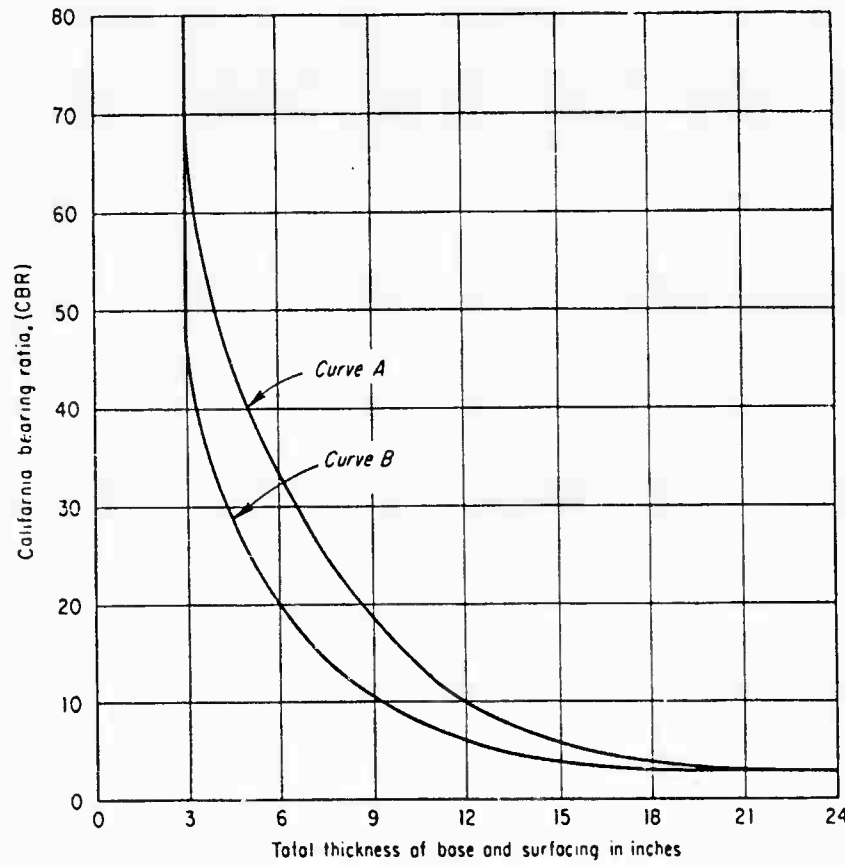


Figure 4-1. Total Thickness of Base and Surfacing in Relation to CBR

The CHD also found that curve A was more reliable and therefore, assumed it to represent a 9,000 lb. wheel load. They also reasoned that because aircraft tires operate at larger deformations and the traffic on airfields is less channelized, this curve would also represent a 12,000 lb. aircraft wheel load (6:424).

Because of the war emergency program, the COE utilized soil mechanics to extrapolate from the 12,000 lb. curve to curves for larger wheel loads. Curves for larger wheel loads were generated based on the assumption that the pavement acted as a homogeneous layer. These tentative design curves are shown in Figure 4-2.

Towards the end of World War II, the U.S. Army Air Corps introduced the B-29 bomber. It complicated flexible pavement design, as it had a dual-wheeled gear. The COE proceeded with an analysis of its effect on flexible pavements and their design. This analysis was based on the fact that a principal cause of pavement failure was strain or deflection. Their investigation and tests concluded that a single-wheel load that produces the same deflection as a multiple-wheel load will produce equivalent or larger strains in the pavement foundation compared to the multiple-wheel load (6:425). This very important concept is known as the equivalent single-wheel load (ESWL) and will be discussed further in section 4.3.

4.3 CBR Thickness Design Procedure

In order to design a flexible pavement using the CBR method, the subgrade CBR, minimum pavement component thicknesses, design aircraft type, and the anticipated traffic volume must all be determined. These variables effect the magnitude and distribution of loads, as well as the frequency that the pavement and subgrade will be subjected to stresses.

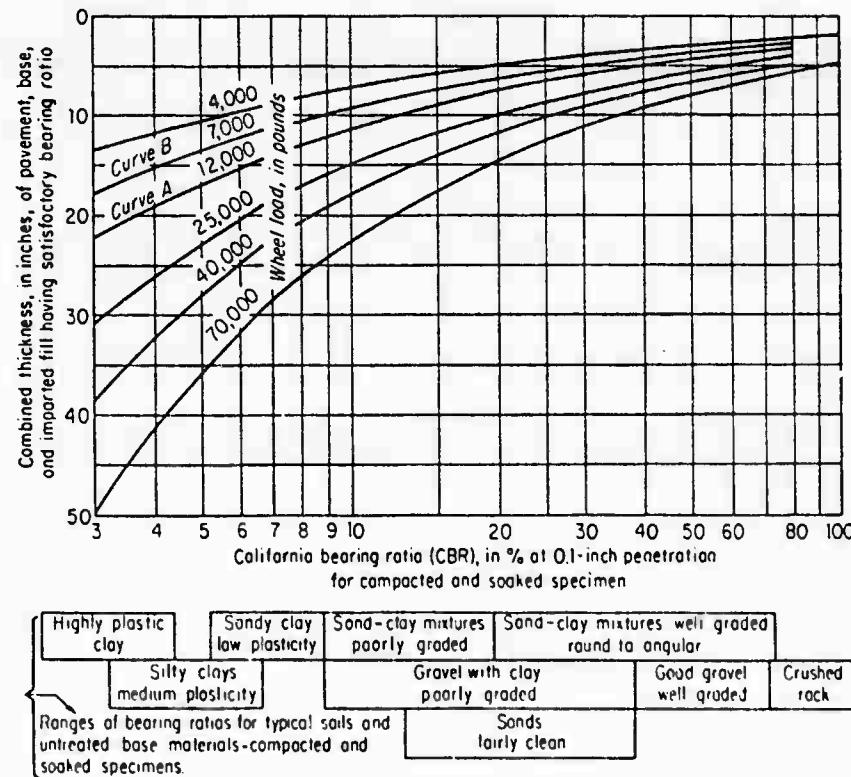


Figure 4-2. Tentative CBR Design Curves

The COE CBR design method is the basis for design methods used by the Navy, Air Force, and Army. They are all quite similar. However, each of these military services uses slightly different design criteria due to the varying ranges of aircraft size and landing gear configuration. The Air Force criteria for flexible airfield pavement design appears to be the most general. This is probably due to the very wide range of aircraft that regularly use Air Force airfields. Their aircraft inventory ranges from the single engine Cessna to the enormous C-5A Galaxy. For this reason, Air Force criteria such as pavement thickness minimums and subbase gradation requirements will be utilized in the design.

4.3.1 Subgrade and Subbase Design CBR Selection

The CBR design procedure may be considered to be empirical and acquires its validity through the correlation of lab or field (in-situ) CBR test values with known traffic loadings and frequencies. When various soil types are encountered at the site, a range of subgrade CBR values may be found to exist. Where this condition exists, some designers select the lowest CBR value for pavement thickness determination when the difference in the high and low CBR value is not too large. When lower than average values are found in isolated locations across the site, the designer should consider replacing these areas with more suitable material before constructing the pavement.

The lab determined CBR must also be compared to maximum allowable CBR design values that are determined by the subbase gradation requirements set forth in Table 4-1. For example, suppose that a lab test determined a subbase CBR of 40 and sieve analysis on the same material showed 85% passing the no. 10 sieve. From Table 4-1, the maximum

Table 4-1. Maximum Permissible Subbase CBR Values

Material	Maximum Design CBR	Size (in.)	Maximum Values			
			Gradation Requirements Percent Passing		Liquid Limit	Plasticity Index
			No. 10	No. 200		
Subbase	50	3	50	15	25	5
Subbase	40	3	80	15	25	5
Subbase	30	3	100	15	25	5
Subbase	20	3	—	25 ¹	35 ¹	12 ¹

¹Suggested limits.

allowable design CBR will be 30. All gradation and Atterberg limit requirements listed in Table 4-1 must be met. Exceptions to the gradation requirements are permissible when supported by adequate in-place CBR tests on similar construction that has been in service for several years (11:5-3).

4.3.2 Design Aircraft Selection and Traffic Forecasting

A design aircraft should be selected as a basis for the pavement design. The design aircraft is generally the heaviest or most damaging aircraft that will operate at the airport, or the most frequent user. The design aircraft's weight and landing gear configuration are the primary aircraft characteristics used in the design of flexible airfield pavements utilizing the CBR method.

It is essential in the design of an airfield pavement to have realistic estimates of the future demand to which the airport will be subjected. There is a variety of forecasting techniques available, ranging from subjective judgement to sophisticated mathematical models, that can be used to estimate both the number and mix of aircraft that will utilize the design airfield over its life. A forecast such as this generally results in a specified number of aircraft passes or movements of the ~~design~~ aircraft by converting all aircraft types to equivalent design aircraft loadings. Due to the broad scope of this concept, it will not be discussed in detail in this paper (6:173-177).

4.3.3 Minimum Pavement Thickness

In order to simplify the infinite variety of loading conditions that may exist, the COE has categorized airfields into three major loading

conditions. The categories are heavy-load, medium-load, and light-load. The design gear load for each of these conditions is 265 kips, 100 kips, and 25 kips, respectively. Table 4-2 gives by traffic area the COE minimum acceptable thicknesses for base and wearing courses for each loading condition. The designer should check to insure that all CBR designs meet these minimum thickness requirements.

4.3.4 Determination of the ESWL

As aircraft became larger and heavier, it was realized that their assembly loads were too large to be delivered to the pavement through a single wheel. To better distribute these loads over the pavement surface, multiple-wheel assemblies were developed.

Because reliable design methods have been formulated based on single wheel loadings, complex landing gear arrangements must be equated to a single wheel configuration, or ESWL. The ESWL replaces for computational purposes the effects of a multiple-wheel assembly with the effects of a single wheel assembly. The ESWL may therefore be defined as a fictitious load acting on a single wheel with the same contact area as one tire of the multiple-wheel assembly, and that produces the same deflection as the multiple-wheel assembly at a given depth in the pavement.

Figure 4-3 shows both the multiple-wheel and single-wheel configurations and their respective deflection conditions. The subscript k in Figure 4-3 (a) refers to known conditions under a dual-wheel gear, while the subscript e shown in (b) of the same figure refers to the ESWL loading configuration. The following analysis is also applicable to more complex landing gear configurations.

Table 4-2. Minimum Surface and Base Thickness Criteria

Heavy-Load Design						
Traffic Area	Minimum Thickness (in.) ¹					
	100-CBR Base			80-CBR Base		
	Surface	Base	Total	Surface	Base	Total
A	5	10	15	6	9	15
B	4	9	13	5	8	13
C	4	9	13	5	8	13
D	3	6	9	3	6	9
Access aprons	3	6	9	3	6	9
Shoulders	2	6	8	2	6	8

Medium-Load Design						
Traffic Area	Minimum Thickness (in.) ¹					
	100-CBR Base			80-CBR Base		
	Surface	Base	Total	Surface	Base	Total
A	4	6	10	5	6	11
B	3	6	9	4	6	10
C	3	6	9	4	6	10
D	3	6	9	3	6	9
Access aprons	3	6	9	3	6	9
Shoulders	2	6	8	2	6	8

continued

Table 4-2. (continued)

Light Load Design						
Single wheel, tricycle; contact area, 100 square inches						
Traffic Area	100-CBR Base			80-CBR Base		
	Surface	Base	Total	Surface	Base	Total
B	3	6	9	4	6	10
C	3	6	9	3	6	9
Access aprons	3	6	9	4	6	10
Shoulders	2	6	8	2	6	8
Shortfield Design						
Single-tandem assembly, tricycle; spacing 60 inches center-to-center; contact area, 400 square inches						
Traffic Area	100-CBR Base			80-CBR Base		
	Surface	Base	Total	Surface	Base	Total
A	4	6	10	5	6	11

¹When underlying subbase layer has a design CBR of 80, the minimum thickness of base course is 6 inches.

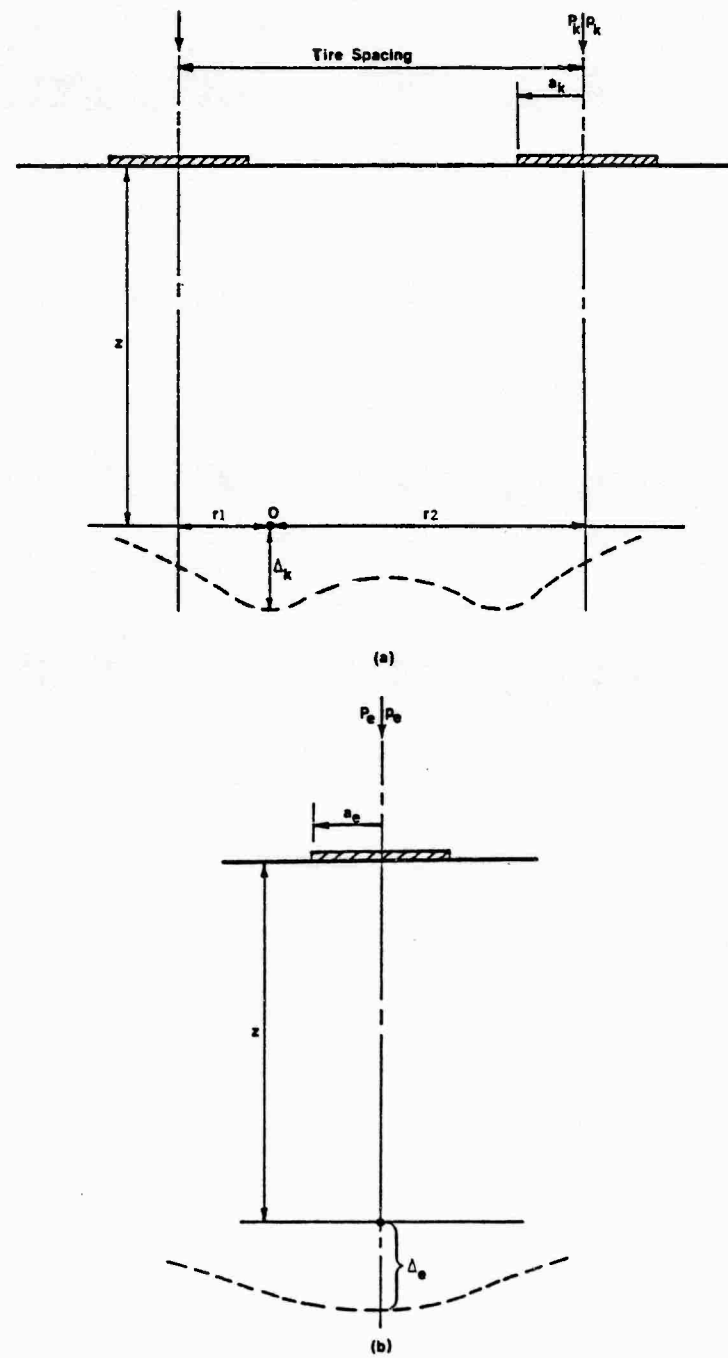


Figure 4-3. ESWL Analysis. (a) Deflection Under Multiple Gear. (b) Deflection Under Equivalent Single Wheel

In Figure 4-3, a_k is the radius of the assumed round, known contact area of one tire for the dual wheel configuration and a_e is the same for the ESWL configuration tire. Horizontal offset distances from each tire in the known configuration to the computational point in question, 0, are represented by r_1 and r_2 .

In an elastic, homogeneous medium, the deflection Δ is expressed as:

$$\Delta = \frac{paF}{E} \quad (4.1)$$

where

Δ = deflection, in.

p = load intensity, psi

a = radius of contact area A_c , in.

E = modulus of elasticity, psi

F = deflection factor obtained from Figure 4-4

In Equation 4.1, the deflection factor, F , is a function of the depth and offset radii ratios.

$$F = f \left(\frac{z}{a} ; \frac{r}{a} \right) \quad (4.2)$$

The total deflection at point 0 for the known multiple gear condition is simply the sum of the deflections contributed by each wheel load. From Equation 4.1 and Figure 4-3:

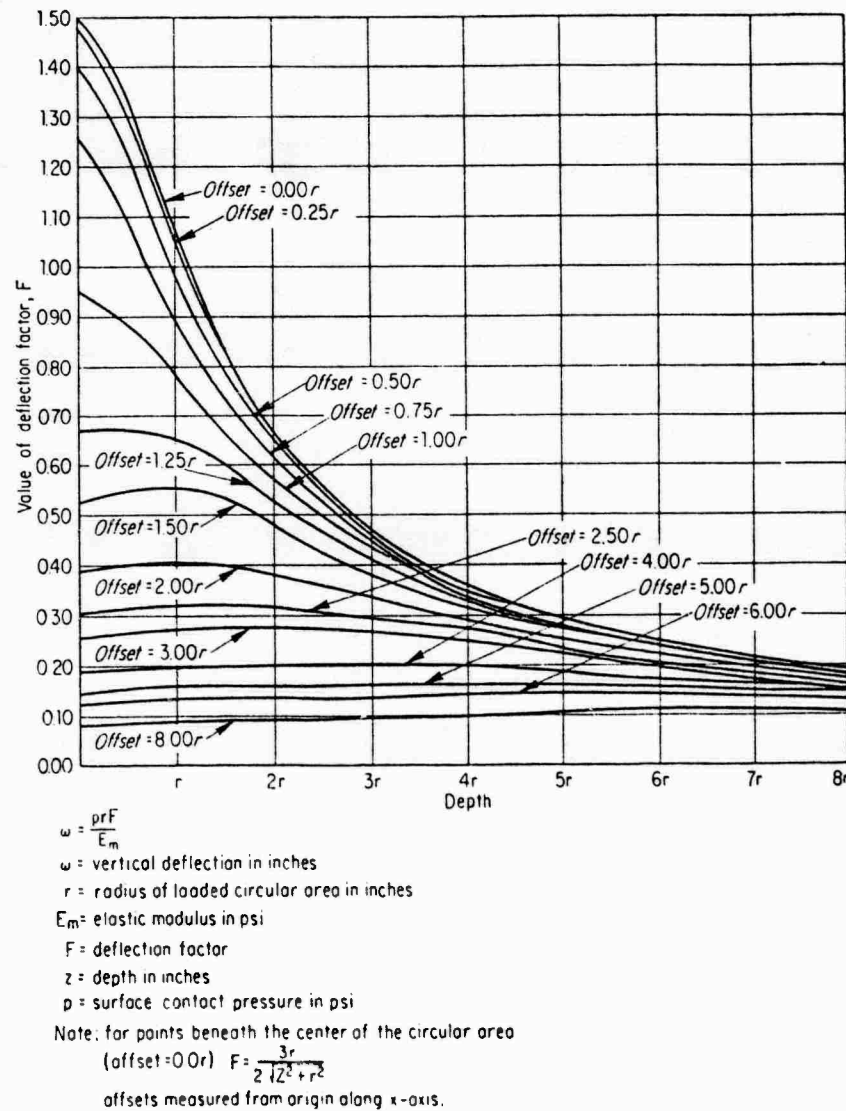


Figure 4-4. Deflection Factor, F , for Uniform Load of Radius r ; Poisson ratio = 0.50

$$\Delta_k = \Delta_1 + \Delta_2 = \frac{p_k a_k}{E} (F_1 + F_2) \quad (4.3)$$

$$\text{where } F = f \left(\frac{z}{a_k}; \frac{r}{a_k} \right) \quad (4.4)$$

Similarly, for the ESWL:

$$\Delta = \frac{p_e a_e}{E} F_e \quad (4.5)$$

$$\text{where } F = f \left(\frac{z}{a_e}; \frac{r}{a_e} \right) \quad (4.6)$$

It is desired that the total deflection under the ESWL equal the total deflection beneath the multiple gear load. Therefore, by equating the two, P_e , or the ESWL, may be solved for. By equating equations 4.3 and 4.5:

$$\left(\frac{p_k a_k}{E} \right) \sum F_i = \left(\frac{p_e a_e}{E} \right) F_e \quad (4.7)$$

Since there are equal tire contact areas, $a_k = a_e$, and

$$\pi a_k^2 = \frac{p_k}{p_k} = \frac{p_e}{p_e} \quad (4.8)$$

Therefore:

$$p_e = \left(\frac{p_e}{p_k} \right) p_k \quad (4.9)$$

Substituting Equation 4.9 into Equation 4.7 gives

$$\left(\frac{p_k a_k}{E} \right) \sum F_i = \frac{p_e p_k}{p_k} \left(\frac{a_e F_e}{E} \right) \quad (4.10)$$

By cancellation of terms and solving for P_e

$$P_e = \frac{P_k \sum F_i \max}{F_e} \quad (4.11)$$

where $F_e = \frac{1.5}{\sqrt{1 + (z/a)^2}}$ (4.12)

For any multiple-wheel assembly, P_k is known. Therefore, the ESWL analysis is simplified to finding the magnitude and location of the maximum $\sum F_i$ value at a specific depth. For dual-wheel gears, $\sum F_i$ values are calculated under one tire and at the center of gravity of the assembly. For dual-tandem assemblies, $\sum F_i$ values are computed underneath the center of one tire, at the center of a line connecting the two closest tires, and at the center of gravity of the assembly. This method of ESWL determination will be illustrated in a case study presented in Chapter Five.

4.3.5 CBR Design Curve Development

The COE has developed a flexible pavement design method that allows CBR versus thickness curves to be generated for any aircraft with any type of landing gear configuration. The design curve can then be used to determine the thickness of pavement required to protect the subgrade. The equations used in this design process were derived from actual data taken from test sections and operational airfields (12:40).

In Chapter Three, it was stated that the design thickness, t , of a pavement is the standard thickness, T , corrected by a load repetition factor, α_i . This standard thickness can be found by using the following equation:

$$T = \sqrt{\frac{ESWL}{8.1 CBR} - \frac{A_c}{\pi}} \quad (4.13)$$

where

ESWL = equivalent single wheel load

CBR = subgrade CBR index

A_c = tire contact area of one tire, in.²

Equation 4.13 may also be expressed as:

$$\sqrt{\frac{T}{A_c}} = \sqrt{\frac{1}{8.1 \frac{CBR}{p_e}} - \frac{1}{\pi}} \quad (4.14)$$

where

p_e = ESWL tire pressure, psi

Note that Equation 4.14 is expressed in terms of the two parameters, $\frac{T}{A_c}$ and $\frac{CBR}{p_e}$.

Equation 4.13 has one very significant limitation. It is only valid for CBR values of up to about 15. Because of this, further tests were conducted by the COE Waterways Experiment Station that resulted in a new equation and a new $\frac{CBR}{p_e}$ versus $\sqrt{\frac{T}{A_c}}$ relation. The statistical equation of the best-fit curve from collected data is:

$$\sqrt{\frac{T}{A_c}} = -0.0481 - 1.562 \log \left(\frac{CBR}{p_e} \right) - 0.6414 \log \left(\frac{CBR}{p_e} \right) - 0.4730 \log \left(\frac{CBR}{p_e} \right) \quad (4.15)$$

Note that Equation 4.15 is also expressed in terms of $\frac{T}{A_c}$ and $\frac{CBR}{p_e}$. These

parameters were plotted as a combined CBR curve using actual performance data obtained and is shown in Figure 4-5. Equation 4.15 and the curve in Figure 4-5 are valid for any CBR. With this in mind, the following steps outline the procedure for generating a CBR versus thickness curve for any type of aircraft with any landing gear configuration.

- Step 1. Assume a series of design thicknesses at which corresponding CBR values will be calculated. A good interval to use is every 10 inches to 70 inches of depth.
- Step 2. Convert the design thicknesses assumed in step 1 above to standard thicknesses using the load repetition factors found in Figure 3-3. These factors are based on the number of anticipated aircraft passes and the number of main landing gear tires used to calculate the ESWL.
- Step 3. Divide the standard thicknesses found in Step 2 by the square root of the area of tire contact. Enter Figure 4-5 with each $\frac{T}{\sqrt{A_c}}$ value to determine corresponding $\frac{CBR}{p_e}$ values.
- Step 4. Determine the ESWL at each of the depths or thicknesses assumed in Step 1. Divide each ESWL by the contact area of one tire to obtain the ESWL tire pressure (p_e).

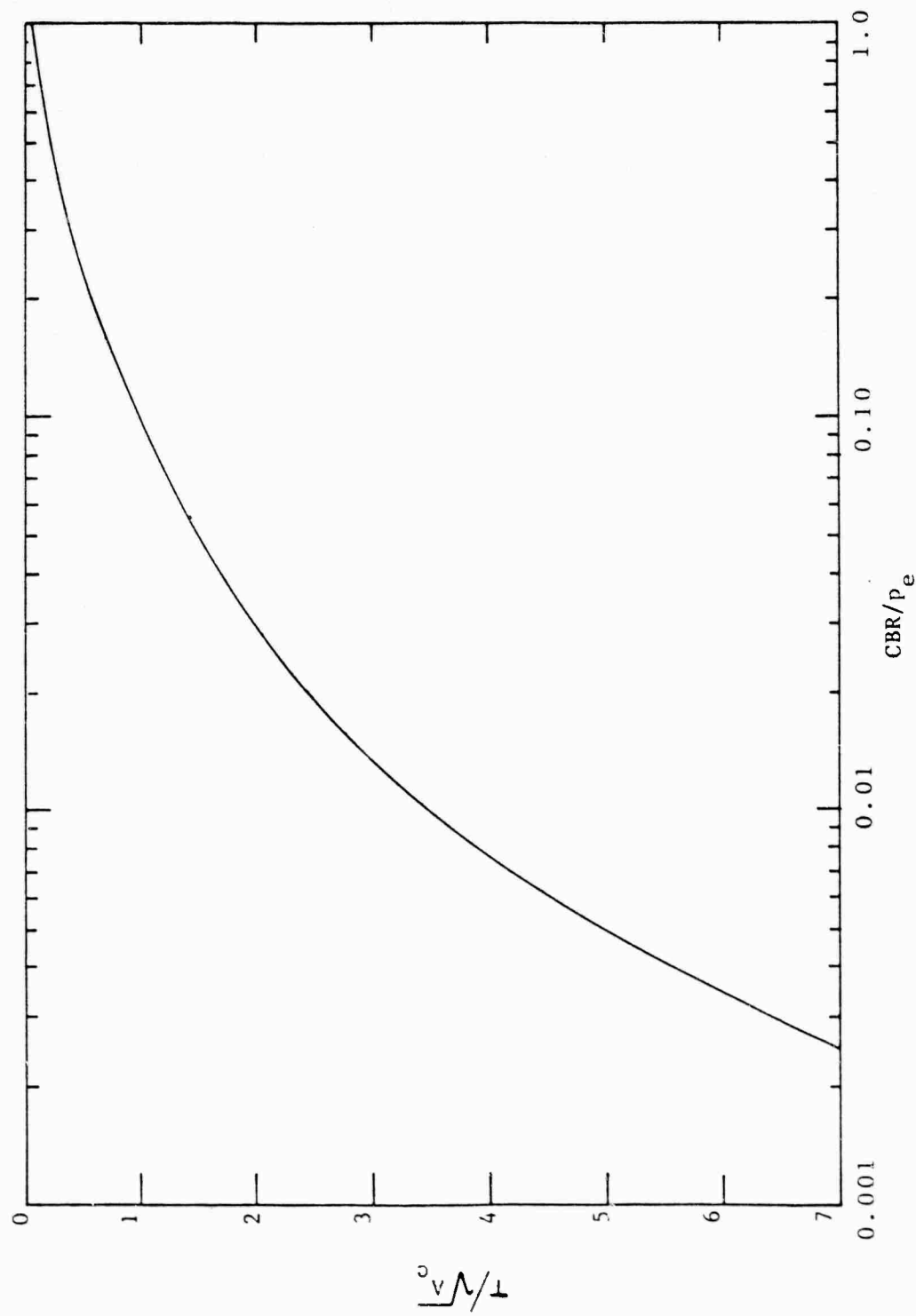


Figure 4-5. $\frac{T}{A_c}$ versus $\frac{CBR}{P_e}$

Step 5. Multiply each of the $\frac{CBR}{p_e}$ values found in Step 3 by the corresponding p_e value determined in Step 4 to obtain the CBR value required below each assumed thickness.

Step 6. Plot each determined CBR value against the corresponding design thickness on a semi-log plot.

Figure 4.6 is provided as an example of a CBR versus thickness design curve. This procedure and the use of the resulting design curve will be demonstrated as part of a case study presented in Chapter Five.

4.4 Design for Protection Against Frost

Severe frost action can result in the nonuniform heave of pavements during the winter and spring months because of ice segregation or the loss of supporting capacity during thawing. During the winter, ice lenses are formed in the subgrade voids. As the temperature begins to rise in the spring and summer, the upper ice lenses in the subgrade begin to melt first. Because the deeper ice has not yet thawed, there is no place for the melting ice to drain. This lack of drainage results in a loss of strength in the subgrade (6:466).

Some soils are more susceptible to frost than others. The COE has classified soils according to their susceptibility to frost, as shown in Table 4-3.

Two methods of frost design have been developed by the COE. The first method provides a sufficient thickness of pavement to insulate the subgrade. The second method allows for the freezing of the subgrade and produces a pavement thickness on the basis of a reduced pavement

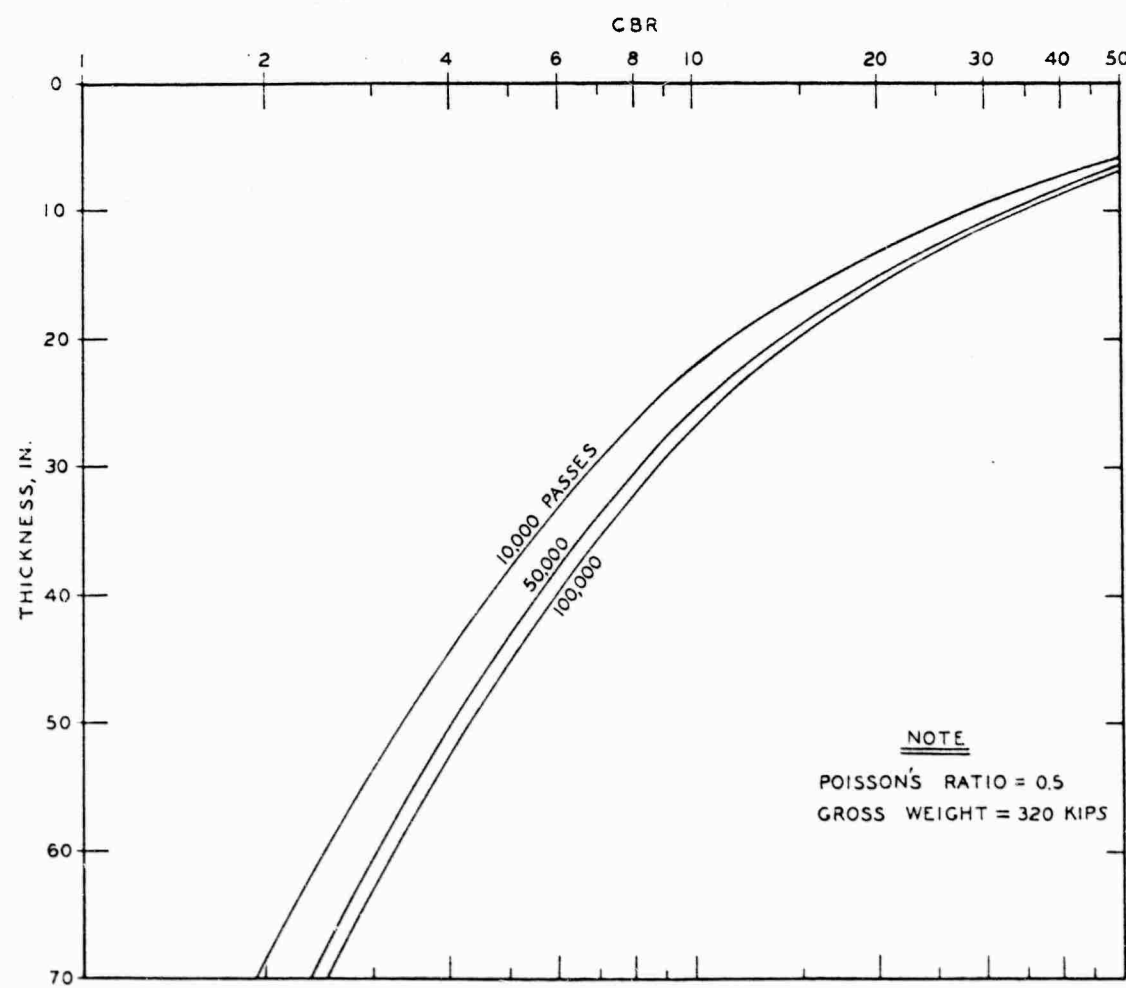


Figure 4-6. CBR/thickness Design Curves for the C-141 Aircraft

Table 4-3. Frost Susceptibility Classification of Soils

Frost Group	Degree of frost susceptibility	Type of soil	Percentage finer than 0.02 mm by weight	Typical soil classification
F1...	Negligible to low.	Gravelly soil	3 to 10....	GW, GP, GW-GM, GP-GM.
F2...	Low to medium.	Gravelly soils Sands.....	10 to 20 .. 3 to 15....	GM, GW- GM, GP-GM. SW, SP, SM, SW-SM, SP-SM.
F3...	High....	Gravelly soils Sands, except very fine silty sands	Greater than 20 Greater than 15	GM-GC. SM, SC.
F4...	Very high	Clays PI >12 All silts Very fine silty sands. Clays, PI <12 Varved clays and other fine grained, banded sediments. Greater than 15	CL, CH- ML-MH. SM. CL, CL-ML. CL, ML, SM, CH.

strength during the thawing period. The choice of method depends on the subgrade material characteristics, the economics of construction at a particular site, and the allowable amount of nonuniform heave (6:467).

The depths of frost penetration typical of various geographical regions have been correlated to a number known as the freezing index. The freezing index is defined as the number of degree-days between the highest and lowest points on a curve of cumulative degree-days versus time for one freezing season. Such a curve is shown in Figure 4-7. A degree-day is defined as the difference between the average daily temperature and 32 degrees, Farenheit.

The freezing index used for design is related to the coldest winter in a 10 year period, or the average of the three coldest winters over a thirty year period. Figure 4-8 shows the distribution of design freezing index values for the continental United States. The freezing index value acquired from Figure 4-8 can be related to the depth of frost penetration through Figure 4-9, which is a graph of freezing index versus frost penetration (6:466-467).

In the first frost design method, some penetration of the frost into the subgrade is acceptable. From extensive studies, the COE has determined the acceptable amount of frost penetration into the subgrade, which is dependent on the thickness of the base course. This relationship is shown in Figure 4-10 (6:467-468). The x-axis of this figure represents the base thickness for a flexible pavement, assuming no penetration of frost into the subgrade. The base thickness is obtained by subtracting the thickness of the surface course from the depth of frost penetration found in Figure 4-9. The y-axis gives the frost design thickness of the

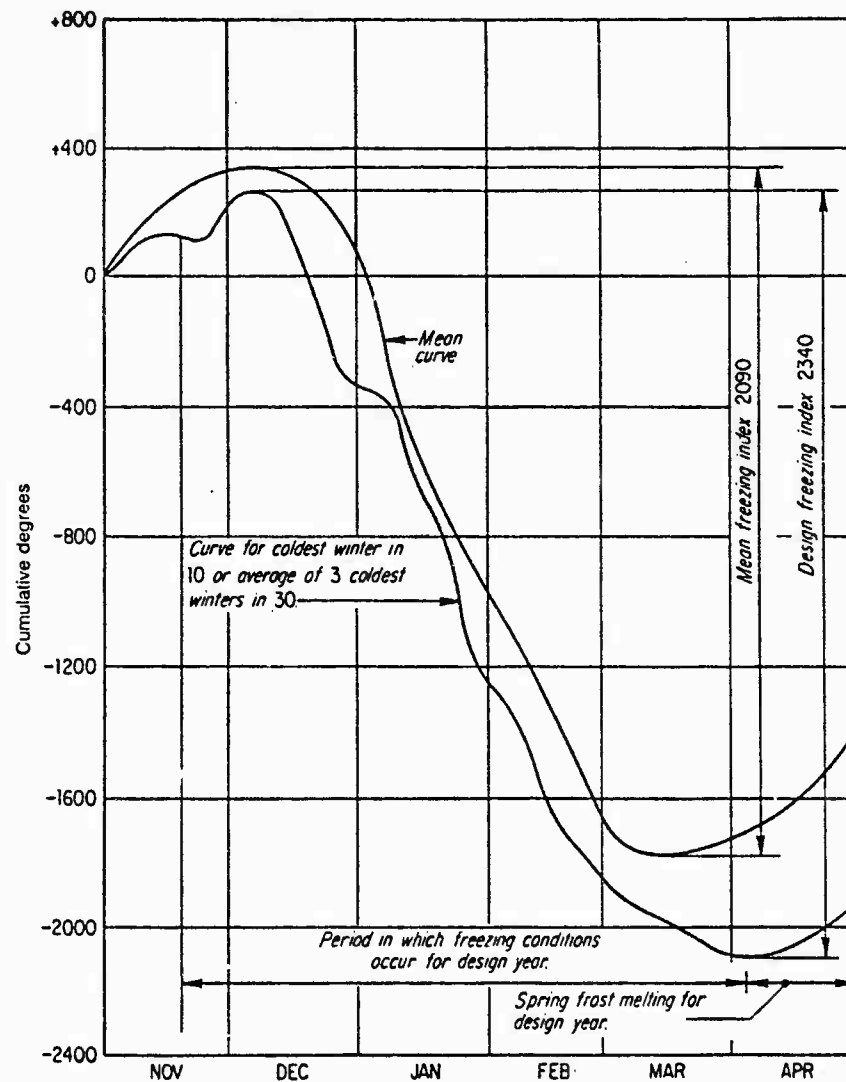


Figure 4-7. Determination of Freezing Index

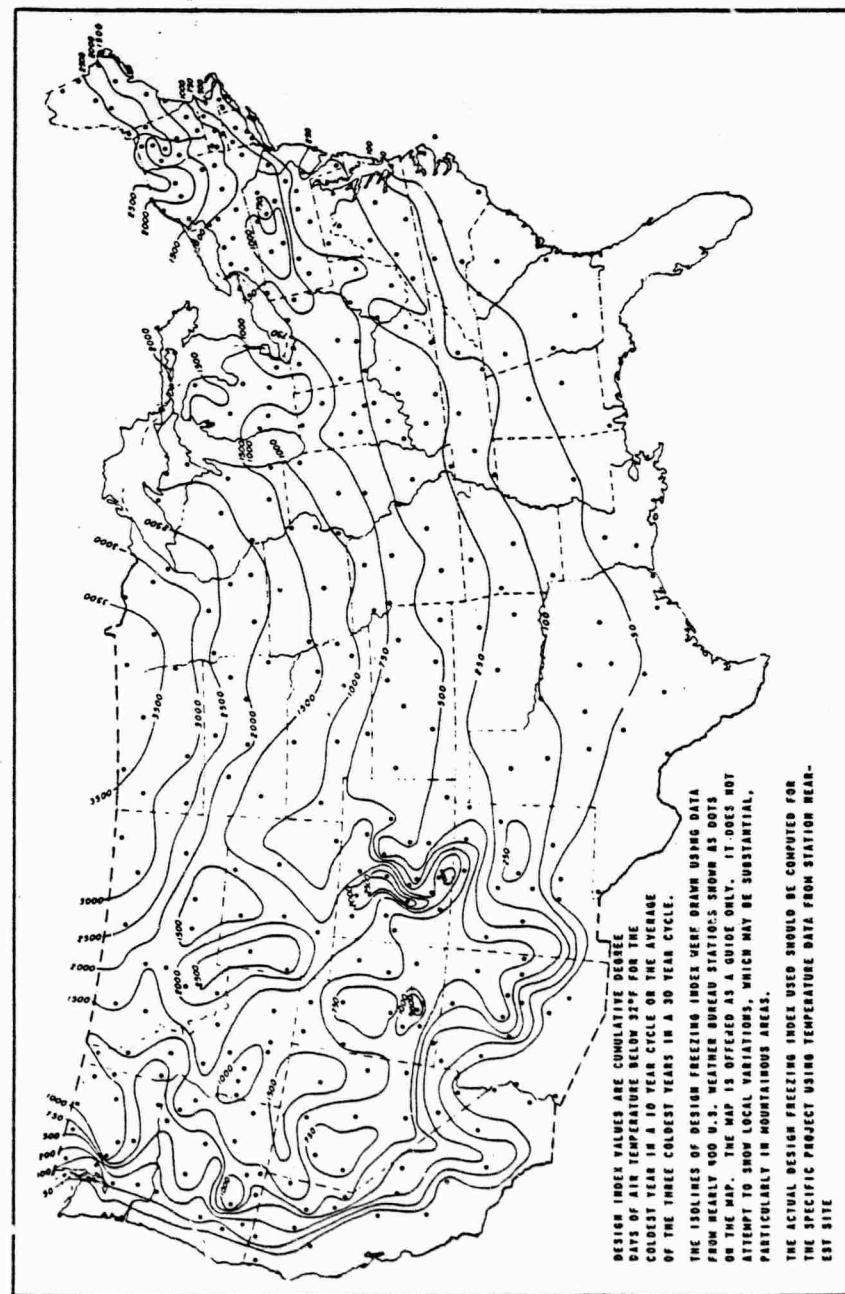


Figure 4-8. Distribution of Design Freezing Index Values in the Continental United States

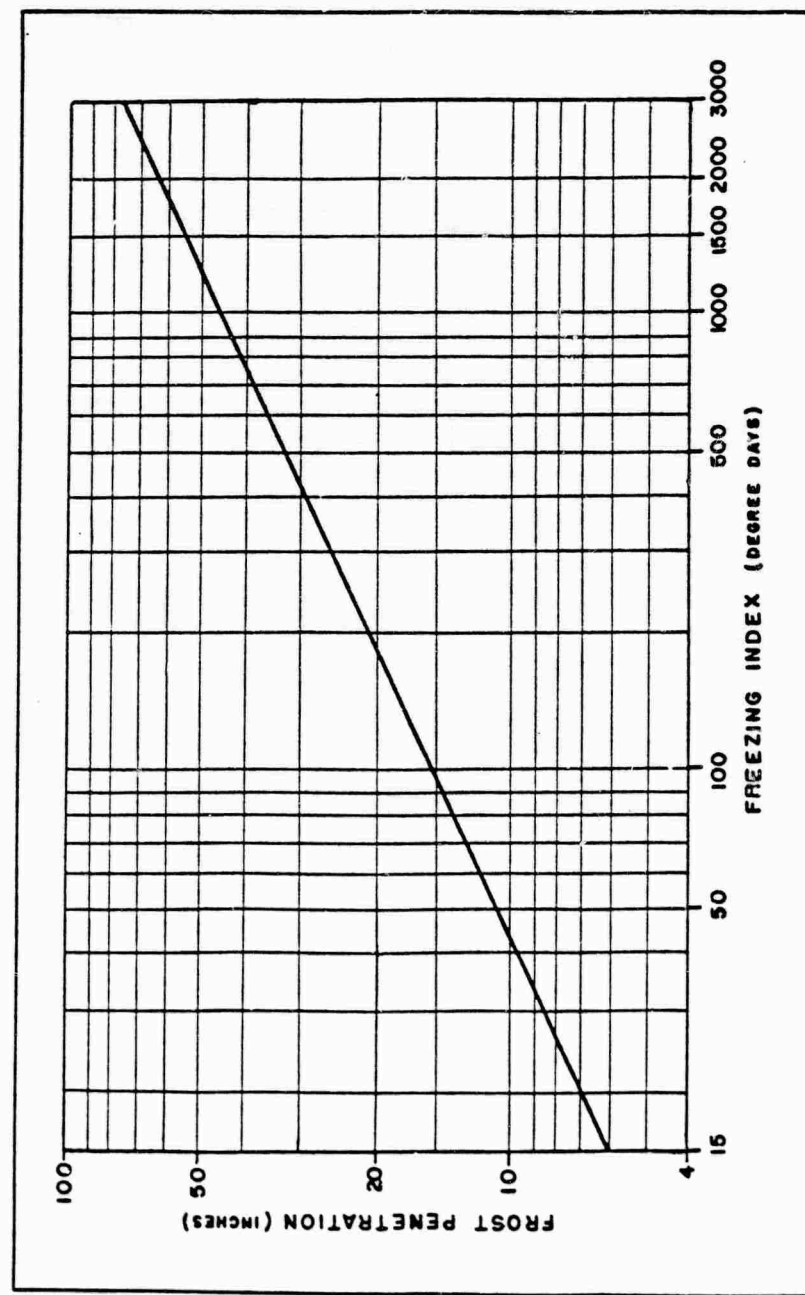


Figure 4-9. Freezing Index Versus Frost Penetration

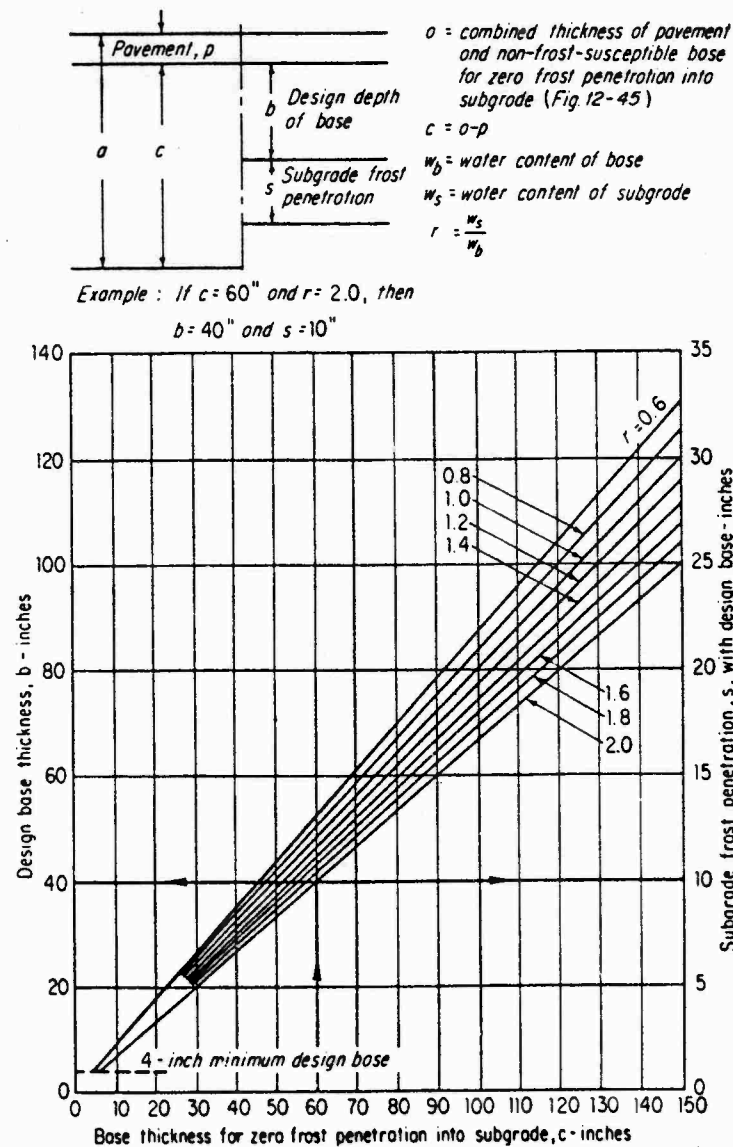


Figure 4-10. Design Depth of Non-frost-susceptible Base for Limited Subgrade Frost Penetration

base and the acceptable depth of frost penetration into the subgrade. The pivot line are based on values of r , which is a ratio of the subgrade water content to the base water content.

The pavement thickness determined from the method described above should then be compared to the design thickness determined from CBR design curves, with the larger of the two thicknesses being used.

In the second method, design diagrams have been developed for flexible pavements that relate landing gear assembly loads and configurations to pavement thickness for each of the frost groups shown in Table 4.3. Figure 4-11 shows a typical design chart for a particular landing gear configuration. Note that F4 soils are not included in this chart. This procedure is normally not applicable to these types of soils, as they can result in nonuniform heave (6:469). The first frost design method described above should be used for F4 soils.

As with the first method, the thickness determined from Figure 4-11 should be compared to the design curve determined thickness, with the larger of the two being used for design.

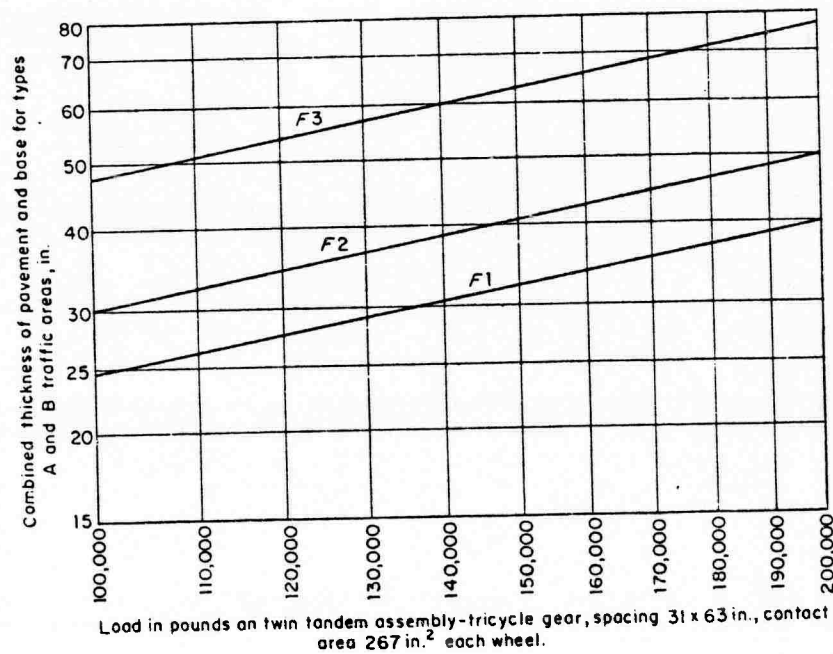


Figure 4-11. Frost Condition; Reduced Subgrade Strength Design Curves for Flexible Pavements

CHAPTER FIVE

CASE STUDY: PALAU AIRFIELD

5.1 Introduction

The Republic of Palau is a Micronesian archipelago nation located in the southwest Pacific Ocean about 700 miles due southwest of Guam (Figure 5-1). It is a former District of the Trust Territory of the Pacific Islands (TTPI). The TTPI was created by the United Nations at the end of World War II, with the United States assuming the role of administrator, as directed by the United Nations (4:6-7).

The Palau Islands had a combined population of about 15,000 in 1983. There are approximately 200 islands in the archipelago, with most of the 15,000 people being concentrated on the district center island of Koror as shown in Figure 5-2 (4:6-7).

In the 1970's, the United States Navy undertook a construction effort known as the Capital Improvement Program (CIP). The basic mission of the CIP was to provide the districts of the TTPI (Palau, Yap, Truk, Ponape, Marianas, and Kosrae) with basic infrastructure that would help these tiny island groups to catch up with the rest of civilization. The focal point of the construction effort in each of the TTPI districts was the construction of a new airfield (9:10).

This chapter will present a case study concerning the design and construction of a flexible pavement airfield in the Palau Islands. The case study will first give pertinent background information concerning the project in general, and will discuss the area geography and climate.

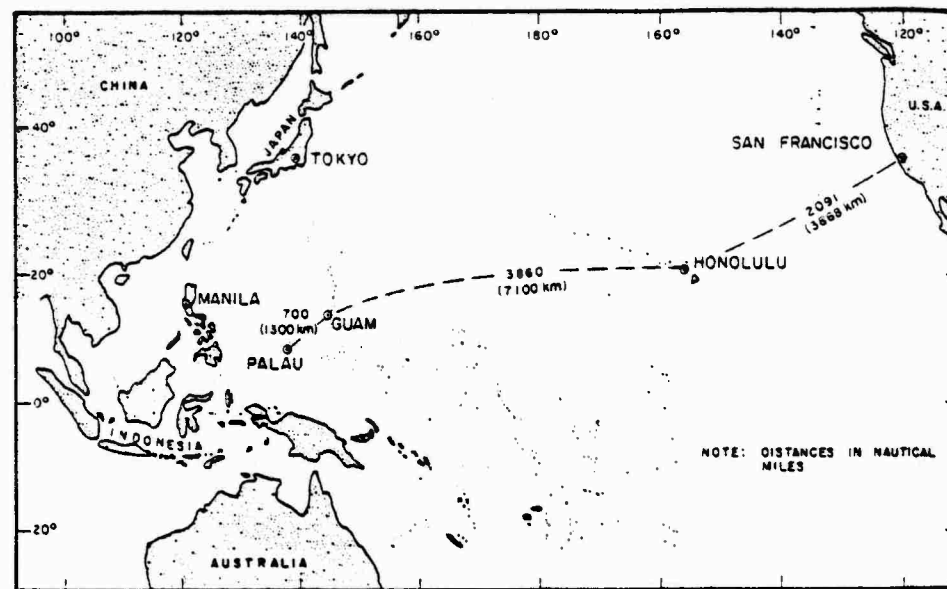


Figure 5-1. Palau and Its Neighbors

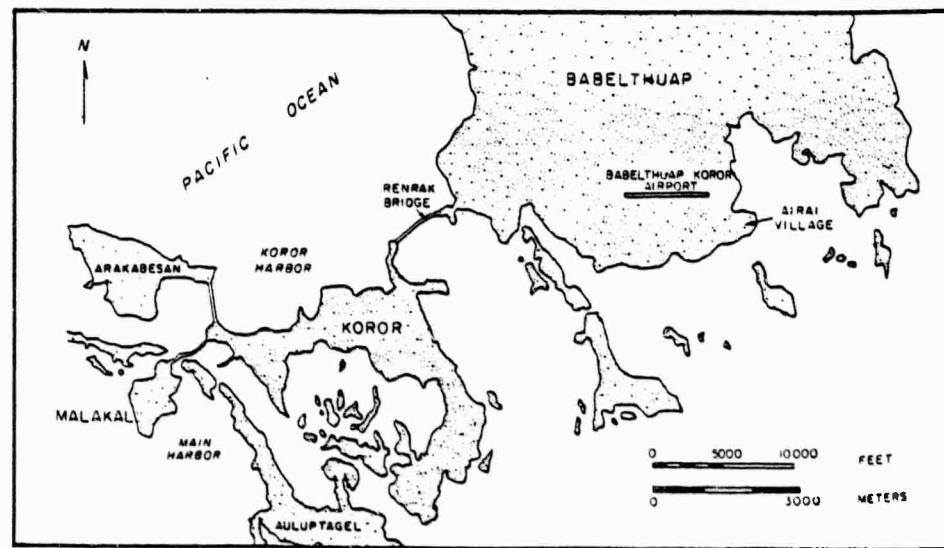


Figure 5-2. Area Map

Section 5.2 will review the design criteria used and discuss the actual design as accomplished using the Federal Aviation Administration (FAA) design method for flexible airfield pavements.

Section 5.3 will present a design based on the same criteria using the COE CBR design method. This design will be compared to the actual FAA design in section 5.4.

It should be stressed that the purpose of section 5.2 is not to investigate the FAA design method, but rather to present its design product to make it available for the comparison mentioned above.

5.1.1 Palau Climate and Geology

Palau has nine months of very heavy rainfall, with the other three being quite dry. On the average, there is about 150 inches of rainfall per year. The temperature rarely fluctuates lower than 81°F. or over 89°F. The relative humidity is always high, averaging about 82 percent (9:10).

The upper soils on Palau are evidently the result of a long period of intense weathering. The dominant weathering processes have been a reduction in organics, rain leaching and atmospheric oxidation (5:4). Almost all of the silicates have been removed from the soil, making the residual soil truly lateritic. The soil in Palau is quite red, due to the presence of a small amount of iron oxide.

Subsurface soil conditions at the airfield were found to be fairly consistent across the airfield site. This soil, a red to red brown residual silt, ranges in thickness from about 25 feet to over 60 feet. The residual silt changes to a silty sand with a greenish tint with increasing depth. This layer is typically 15 feet thick and transitions

to a hard, well-cemented, volcanic breccia with a greenish tint. This tint is the result of hydrothermal action subsequent to its formation (5:4).

The strength of the silt at the airport site is fairly consistent, ranging from medium-stiff to stiff. It has an average dry density of 57 PCF and an average moisture content of 75 percent. The average plasticity index is 36 and the average liquid limit is 94. After being oven dried and compacted to 100 percent relative density, this soil displays an average maximum dry density of about 86 PCF and an average optimum moisture content of about 30 percent. Field CBR tests resulted in a range from 3 to 11, with the average being about 5. Most of the near surface soil was saturated due to the high quantity of rain (5:4).

5.2 Palau Airfield Design

5.2.1 Existing Airfield and Design Parameters

The original airstrip was constructed by the Japanese prior to World War II by cutting down several hilltops and filling the intervening valleys. Several modifications had been made since the war, with the final change being an extension from 5,000 feet to 6,000 feet. The existing runway was quite irregular in profile, with the runway ends having a difference in elevation of 20 feet. Figure 5-3 shows the pre-construction runway, looking west. The effective runway width was only 70 to 80 feet in some portions and averaged about 100 feet. Continental Air Micronesia began making regular jet flights to Palau and other TTPI islands from Guam in 1976.



Figure 5-3. Pre-construction Runway, Looking West

5.2.2 New Airfield Design and Construction Criteria

The new runway was to be 7,200 feet by 150 feet, with a 175 foot safety area on each side of the strip. An engineering study was performed to help determine the most suitable location for the new airport. Despite several engineering problems with building on the existing site, this was decided on as the best option. Extending and widening the existing runway would require extensive fill operations, with some fill embankments being 85 to 90 feet. A plan view of the airfield is shown in Figure 5-4. Note that the center 2700 feet of the runway is labeled as full depth asphalt. This is noted for informational purposes only, as this section was designed using the Asphalt Institute's method of design for full depth asphalt pavements. All other areas of the runway, taxiway, and apron were designed by the FAA method and are the topic of discussion here.

Hawaii Architects and Engineers of Honolulu was the design firm selected by the U.S. Navy to design a major portion of the Palau CIP infrastructure, including the Palau airfield. The following are the major criteria used to design the airfield pavement using the FAA method (3):

- (a) FAA design method
- (b) Boeing 727-200, design aircraft
- (c) subgrade CBR of 5
- (d) subbase CBR of 35
- (e) base CBR of 100
- (f) traffic volume of 8000 annual departures, 20 year life.

Note that the FAA design is based on departures instead of coverages or passes.

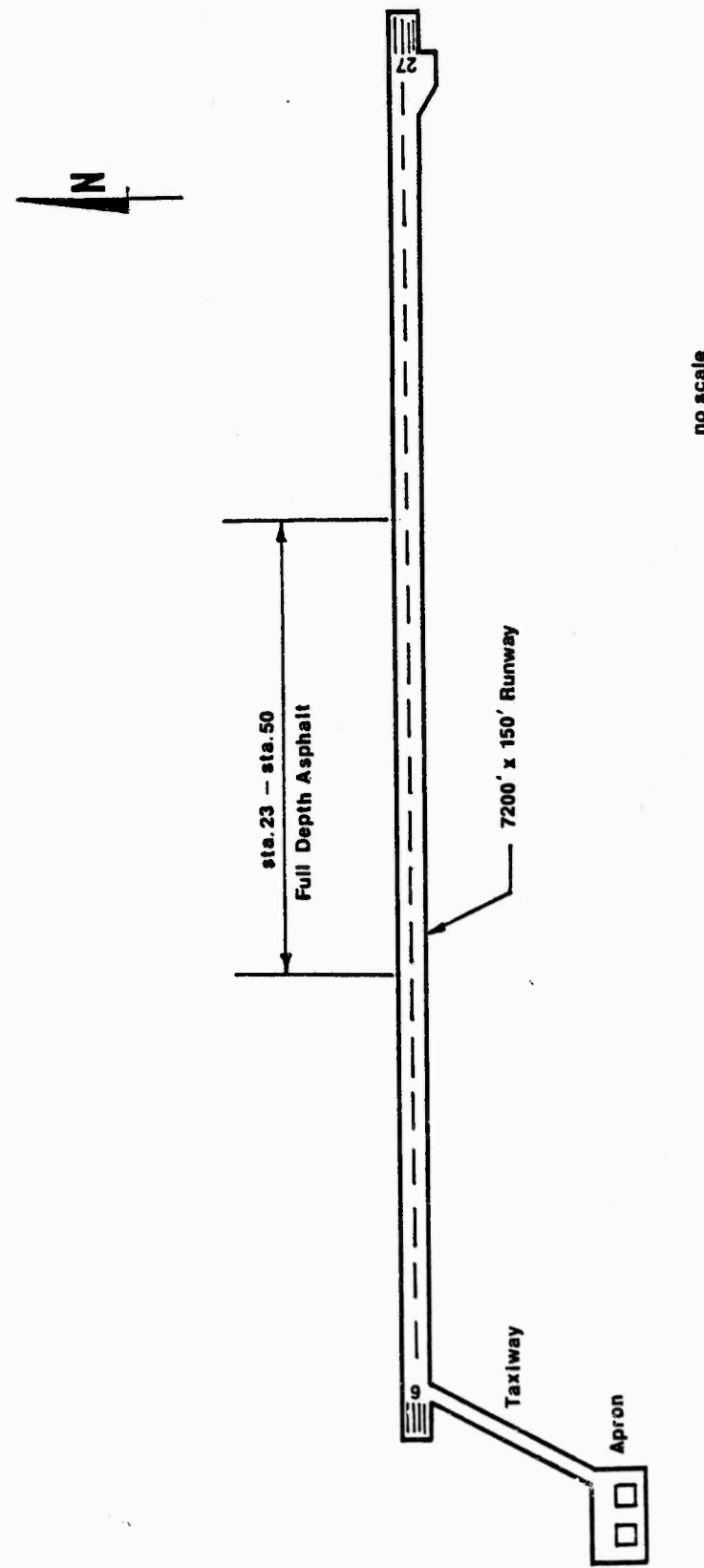


Figure 5-4. Plan View, Palau Airfield

5.2.3 Palau Airfield, FAA Design

Figure 5-5 shows the resulting typical airfield design cross-section for all pavement areas except the full depth section. Figure 5-6 shows the airfield at 99% complete. Note the two concrete hardstands on the apron for aircraft parking.

The asphalt wearing course consists of hot mix asphaltic concrete. The rock base course is crushed basalt that was quarried locally by the contractor, and the subbase course is composed of dredged coral aggregate.

The design cross-section depicted in Figure 5-5 is slightly different than the as-built cross-section. The only difference in the two is that the as-built cross-section has a 10 inch cement modified base, whereas the original design called for a 12-inch non-treated base. This modification was made after construction had begun, and was due to a higher than anticipated plasticity index of the basalt aggregate. The base was treated with 3 percent cement and due to resulting CBR's in excess of 100, the A/E allowed a reduction in this layer from 12 to 10 inches.

5.2.4 Performance of the Palau Airfield

The construction of the Palau airfield was completed in June of 1983. However, there were portions of the pavement that were completed and put into service up to one year prior to this time. The pavement has performed exceptionally well. No load induced distress has been noted to date. Some minor tension cracking has occurred, and are thought to be caused by localized subgrade settlement (3).

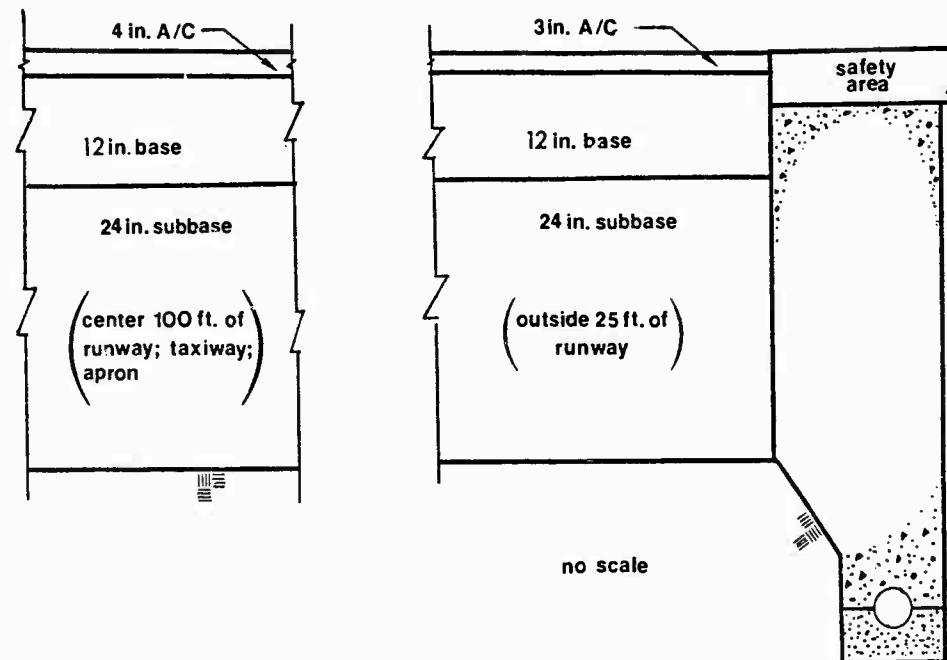


Figure 5-5. Palau Airfield Pavement, FAA Design



Figure 5-6. Palau Airfield, 99% Complete

The 8000 annual departures designed for is far from being realized. There have been about 500 departures per year, average, since the airfield was opened to traffic. Therefore, the pavement is not being truly tested (3).

5.3 Palau Airfield CBR Design

The following will be a complete CBR pavement design for the Palau airfield. The design will be accomplished using the COE CBR design method and will be based on the same criteria as discussed in section 5.2 for the actual FAA design.

The design will first discuss four key parameters for a CBR design: (a) design CBR of subgrade and subbase materials, (b) minimum pavement component thicknesses, (c) design aircraft characteristics, and (d) the forecasted annual aircraft operations.

As discussed in section 4.3, this design will include a demonstration of the ESWL calculations for the design aircraft. This will be followed by the culmination of a CBR design, the development of the CBR versus thickness curves for the design aircraft. The design curves will then be used to determine the thickness of each pavement layer. A comparison of the resulting CBR design will then be made to the FAA design product.

5.3.1 Design Criteria

5.3.1.1 Subgrade CBR Design

As mentioned in section 5.1.1, laboratory CBR determinations made on the subgrade material showed values ranging from 3 to 11, with an average value of 5. The A/E based his design on a subgrade CBR of 5 with the requirement that the contractor remove areas

showing CBR values lower than 5, and replace the material with more suitable material. The Palau airfield CBR design will also be based on subgrade CBR of 5.

5.3.1.2 Subbase and Base Design CBR Values

Laboratory CBR tests performed on the coral aggregate that was used for subbase construction resulted in a CBR of 35 (3). The gradation and Atterberg limits data on this same material is as follows:

- (a) 3 inch maximum size
- (b) 55% passing the no. 10 sieve
- (c) 12% passing the no. 200 seive
- (d) unknown liquid limit
- (e) non-plastic (PI = 0)

Using this data with Table 4-1, it can be determined that the maximum permissible CBR is 40. However, because the laboratory value is only 35, the design CBR for the subbase will be 35. The value acquired from Table 4.1 cannot be used if it exceeds the laboratory determined value.

The base course will be constructed of locally quarried basalt aggregate. A CBR of 100 was determined in the laboratory from soaked CBR tests performed on this material (3).

5.3.1.3 Minimum Pavement Thickness

In looking at Figure 5-4, it can be seen that the most extreme loading condition will occur when a fully loaded aircraft departs and, due to a westerly wind, must take off to the west. This results in a fully loaded aircraft having to taxi the full length

of the runway before turning around to take off. Because the runway will have to be used as a taxiway in this fashion, the inner most 100 feet of the full length of the runway will be designed as a type "A" traffic zone. Of course, the taxiway and apron will also be designed as type "A" traffic areas. The outermost 25 feet along the runway on both sides will be designed as a type "B" traffic zone.

From Table 4-2, the minimum type A pavement thicknesses for a medium-load, 100 CBR base airfield are 4 inches for the asphalt layer and 6 inches for the base. For type B traffic areas, the minimum thicknesses are 3 inches of asphalt and 6 inches of base. Figure 5-7 is a plan view of the Palau airfield showing the layout of traffic areas.

With respect to frost, obviously, this will not be a factor in Palau's tropical climate.

5.3.1.4 Design Aircraft

The design aircraft selected by the A/E for the FAA design was the Boeing 727-200. Most jet flights made to Palau are made in this type of aircraft. The CBR design being presented here will also be based on the 727-200. The following data is considered pertinent to the design (6:60-61):

- (a) maximum gross weight, 170,000 lb.
- (b) main landing gear configuration, dual
- (c) tire pressure, 168 psi
- (d) wheel spacing, 34 in.

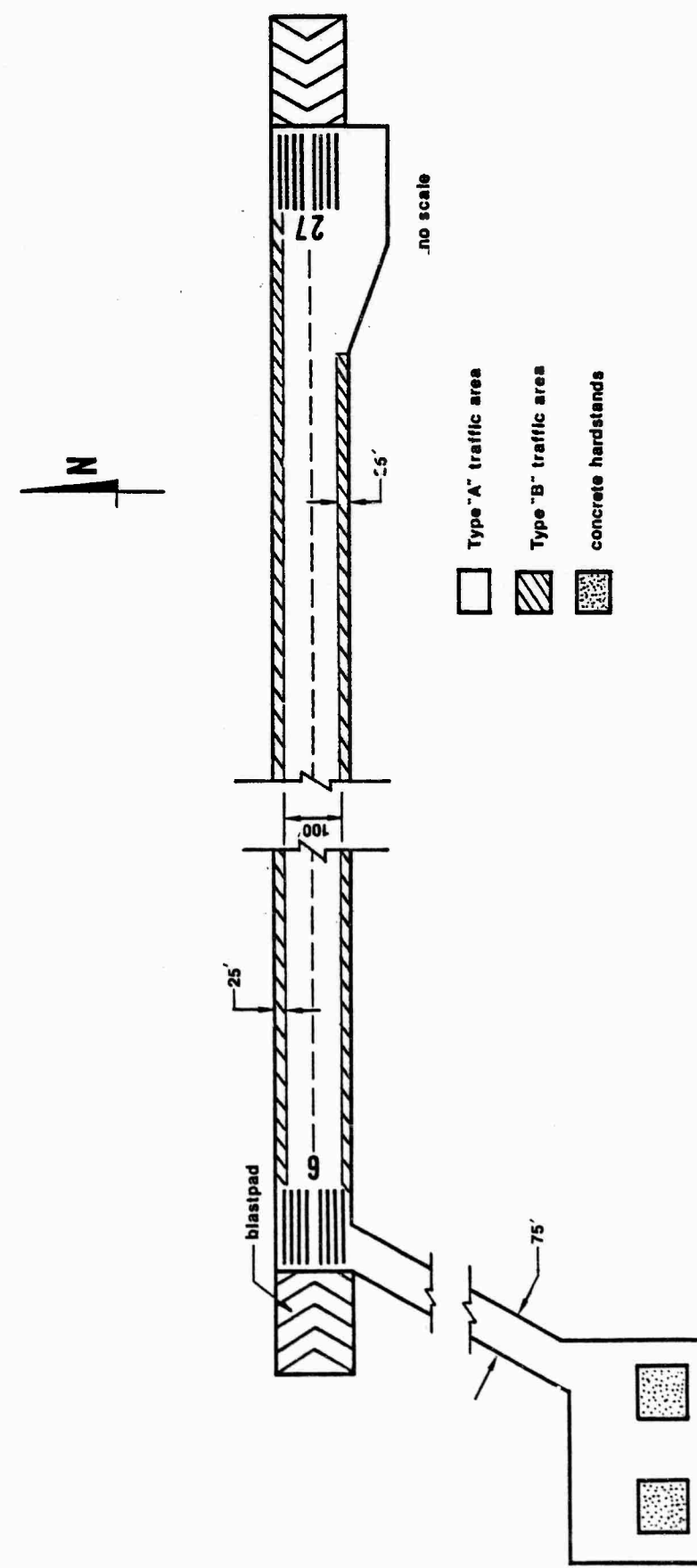


Figure 5-7. Traffic Area Layout, CBR Design, Palau Airfield

A shorter version of the 727-200, the 727-100, is shown landing at the Palau airfield during the construction of the new airfield in Figure 5-8.

5.3.1.5 Forecasted Annual Aircraft Operations

Because the FAA design method is based on the number of annual aircraft departures and the CBR method is based on the number of annual aircraft passes, the two must be equated to each other to insure that both designs are based on the same criteria.

In looking at Figure 5-4, it can be seen that an aircraft can arrive at the airfield from either the east or west. Upon arrival, all aircraft will proceed to the apron, located at the western end of the airfield, for passenger drop-off and pick-up, and servicing. The taxiway and apron will receive two passes per departure. Two passes is equivalent to 2×8000 departures per year for 20 years, or 320,000 passes. Therefore, for type "A" traffic areas, the airfield pavement will be designed for 320,000 passes over a 20 year period.

For type "B" traffic areas, the number of aircraft passes will be reduced. Because type "B" traffic areas are designed for one-fifth the number coverages of type "A" traffic areas, this same factor will be applied to the 320,000 passes being designed for in type "A" traffic areas, resulting in 64,000 passes over a 20 year life for the type "B" areas.

These assumptions and estimates of the frequency of loadings are considered to be valid and close to those that the FAA design was based on.

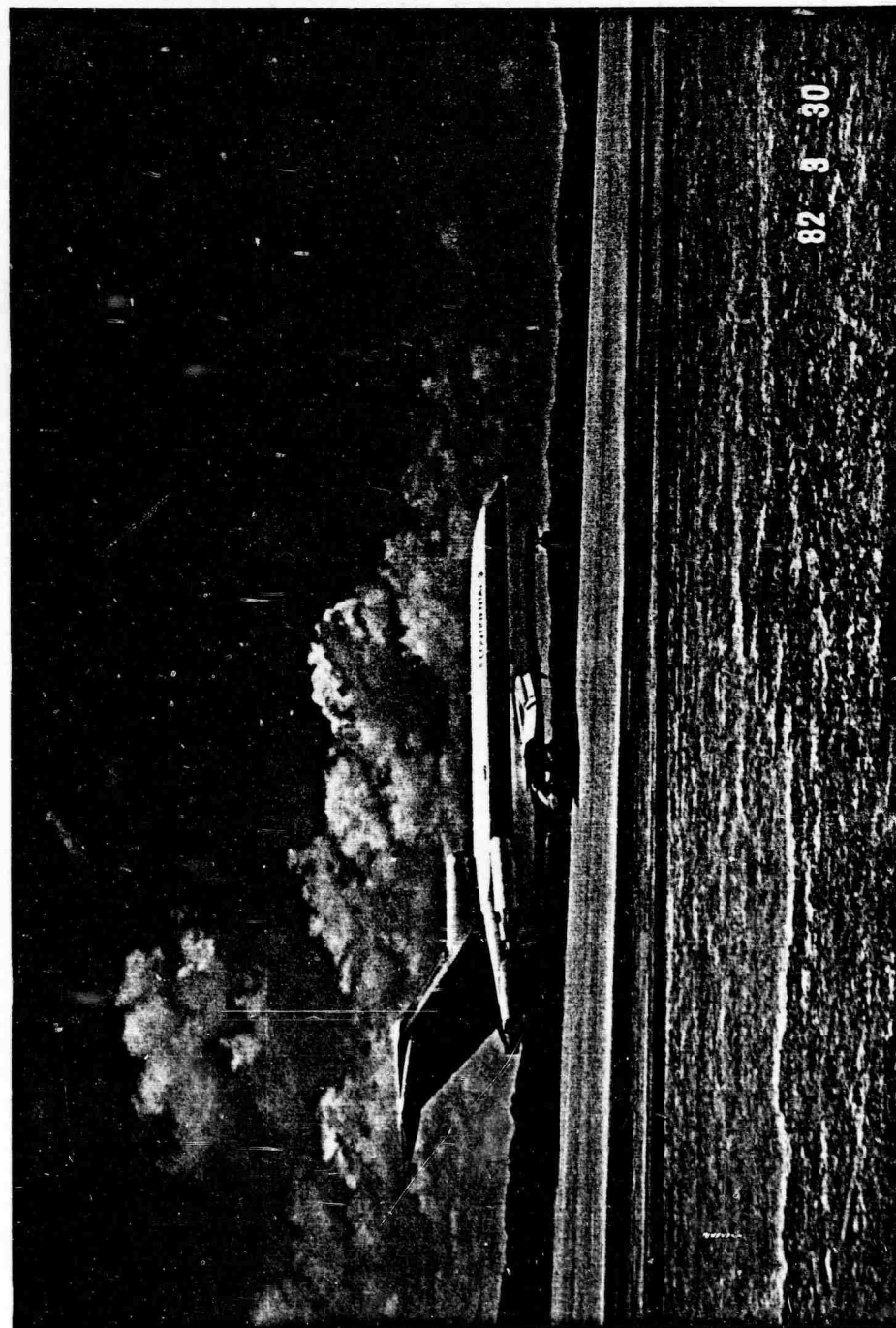


Figure 5-8. 727-100 Landing at Palau Airfield,
Under Construction

5.3.2 ESWL Calculations

Based on the concepts of the ESWL presented in section 4.3.4, the following calculations will demonstrate the procedure for converting multiple-wheel landing gear arrangements to equivalent single wheel loads.

The 727-200 aircraft, as stated, has a dual-wheeled main landing gear configuration. Each main landing gear is assumed to apply 47.5% of the aircraft weight to the pavement. With this in mind, a free-body diagram of one main gear assembly under maximum loading conditions is shown in Figure 5-9.

As shown in section 4.3.4, P , or the load acting on any one tire in a multiple-tire assembly, is known. In this case, $P = 40,375$ pounds, and the area of tire contact is equal to:

$$A_c = \frac{40,375 \text{ lb.}}{168 \text{ psi}}$$

$$= 240 \text{ in}^2$$

The area, A_c , is assumed to equal the area of contact of the ESWL tire and also equal to the area of contact of one tire of the multiple wheel gear. The radius of the assumed round contact area is equal to:

$$a_k = \sqrt{\frac{A_c}{\pi}}$$

$$= \sqrt{\frac{240}{\pi}}$$

$$= 8.7 \text{ in.}$$

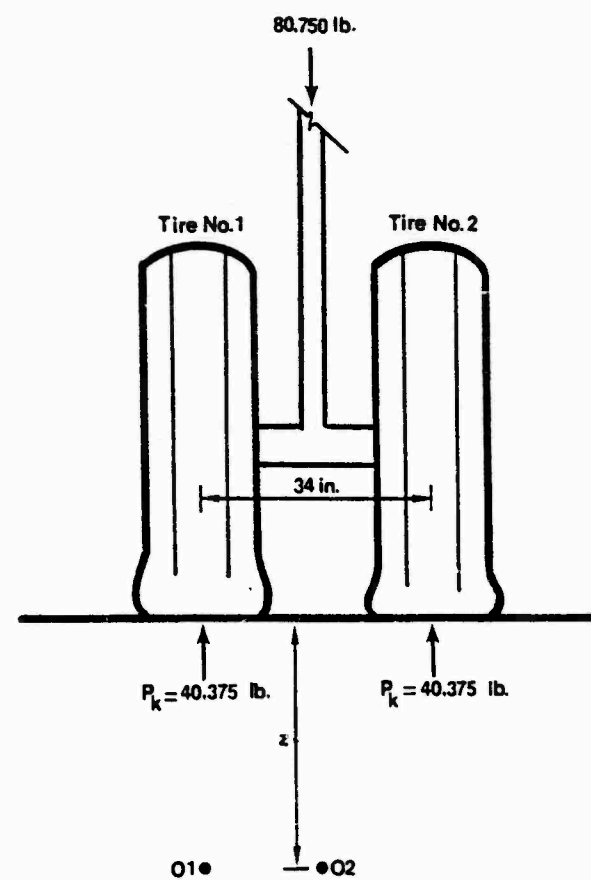


Figure 5-9. Free-body Diagram of Main Landing Gear of 727-200 Aircraft, Fully Loaded

Because we are dealing with a dual-wheel gear, ΣF_i values need to be calculated at the center of gravity of the assembly and directly beneath one tire. The condition resulting in the maximum deflection condition, or the maximum ΣF_i value, is critical and will be used to determine the ESWL at that particular depth. ESWL values will be calculated at 10 inch intervals to a depth of 70 inches. Only the calculation for the ESWL at a depth of 30 inches will be demonstrated.

Again referring to Figure 5-9, points 01 and 02 are the locations where equivalent single wheel loads will be calculated. For clarity, the ESWL calculation at point 01 will be referred to as case 1, and case 2 will refer to the condition at point 02.

Case 1 will be investigated first. The depth below the pavement surface, z , is equal to 30 inches. The offset, r , from tire number 1 to point 01 is equal to zero. The offset from tire number 2 to point 01 is equal to the tire spacing, or 34 inches. With this information, Figure 4-4 can be entered with the depth in radii equal to 30 divided by 8.7, or 3.45. Deflection factors can be found for both tires by using an offset, in radii, of 0 for tire number 1, and an offset of 34 divided by 8.7, or 3.9 for tire number 2. The deflection factors found in Table 4-4 are 0.43 for tire number 1, and 0.21 for tire number 2. Therefore, ΣF_i is equal to the sum of the deflection factors, or 0.64.

For case 2, z is also 30 inches. The offset, r , from tire number 1 to point 02 is equal to 17 inches. The offset from tire number 2 to point 02 is also equal to 17 inches. Therefore, the offset for both tires in radii is equal to 17 inches divided by 8.7, or 1.95 radii. The depth in radii is, again, 3.45. By entering Figure 4-4 with these

values, the deflection factor is found to be 0.33 for tire number 1 and tire number 2. Therefore, the ΣF_i value for case 2 is equal to 0.66. These calculations are summarized in Table 5-1.

From Table 5-1, it can be seen that the maximum ΣF_i value is equal to 0.66 for case 2. This value will be used to calculate the ESWL. The ESWL may now be calculated using Equation 4.11.

$$P_e = \frac{P_k \Sigma F_i \max}{F_e}$$

$$\text{From Equation 4.12, } F_e = \frac{1.5}{\sqrt{1 + (z/a)^2}}$$

$$= 0.42$$

$$\text{Therefore, } P_e = \frac{40,375 (0.66)}{0.42}$$

$$= 63,450 \text{ lb.}$$

The equivalent single wheel load in this case, at a depth of 30 inches, is equal to 63,450 pounds. This fictitious load that is assumed to act on a single wheel produces the same deflection at 30 inches as the dual gear shown in Figure 5-9.

The ESWL value calculated at 30 inches may also be expressed in terms of the percent of assembly load. For example, the 63,450 pound load calculated above is 78 percent of the 80,750 pound assembly load. A graph of depth versus percent of assembly load may be constructed by plotting the percent of assembly load versus depth for ESWL values calculated at various depths. This was done here and is shown in

Table 5-1. ESWL Calculations Summary

	Depth (z/a)	Tire No.		ΣF_t	F_e	P_e (lb) (ESWL)
		1	2			
Case 1	3.45	r/a=0	r/a=3.91	0.64	0.42	61,524
		0.43	0.21			
Case 2	3.45	r/a=1.95	r/a=1.95	0.66	0.42	63,450
		0.33	0.33			

Figure 5-10. This graph may now be used to easily determine the ESWL at any depth up to 70 inches. As will be seen, this curve is quite convenient for constructing CBR versus depth curves.

5.3.3 CBR Design Curve Development

Section 4.3.5 outlined the method for generating CBR design curves for any aircraft loading condition. Once constructed, this curve becomes the main tool used in determining the thickness of each component layer of the pavement being designed.

Tables 5-2 and 5-3 are a summation of the calculations performed for the generation of type "A" and type "B" traffic area design curves, respectively. Both tables follow steps 1 through 6 as outlined in section 4.3.5.

Figures 5-11 and 5-12 are the design curves. They are each a plot of CBR versus thickness curves for the design aircraft operating at 320,000 passes for type "A" traffic areas and 64,000 passes for type "B" traffic areas. Each design curve has been generated by plotting the first and last columns of both Table 5-2 and 5-3. Section 5.3.4 will illustrate the use of these curves.

5.3.4 Pavement Thickness Determination

Now that the design curves have been generated, they can be used to illustrate the thickness determination procedure for the total pavement and each component layer. First, type "A" traffic area pavement thicknesses will be determined.

The total pavement thickness is controlled by the strength, or CBR, of the subgrade. By entering Figure 5-11 with the subgrade CBR of 5, a total pavement thickness of 38 inches is found. This is the total design

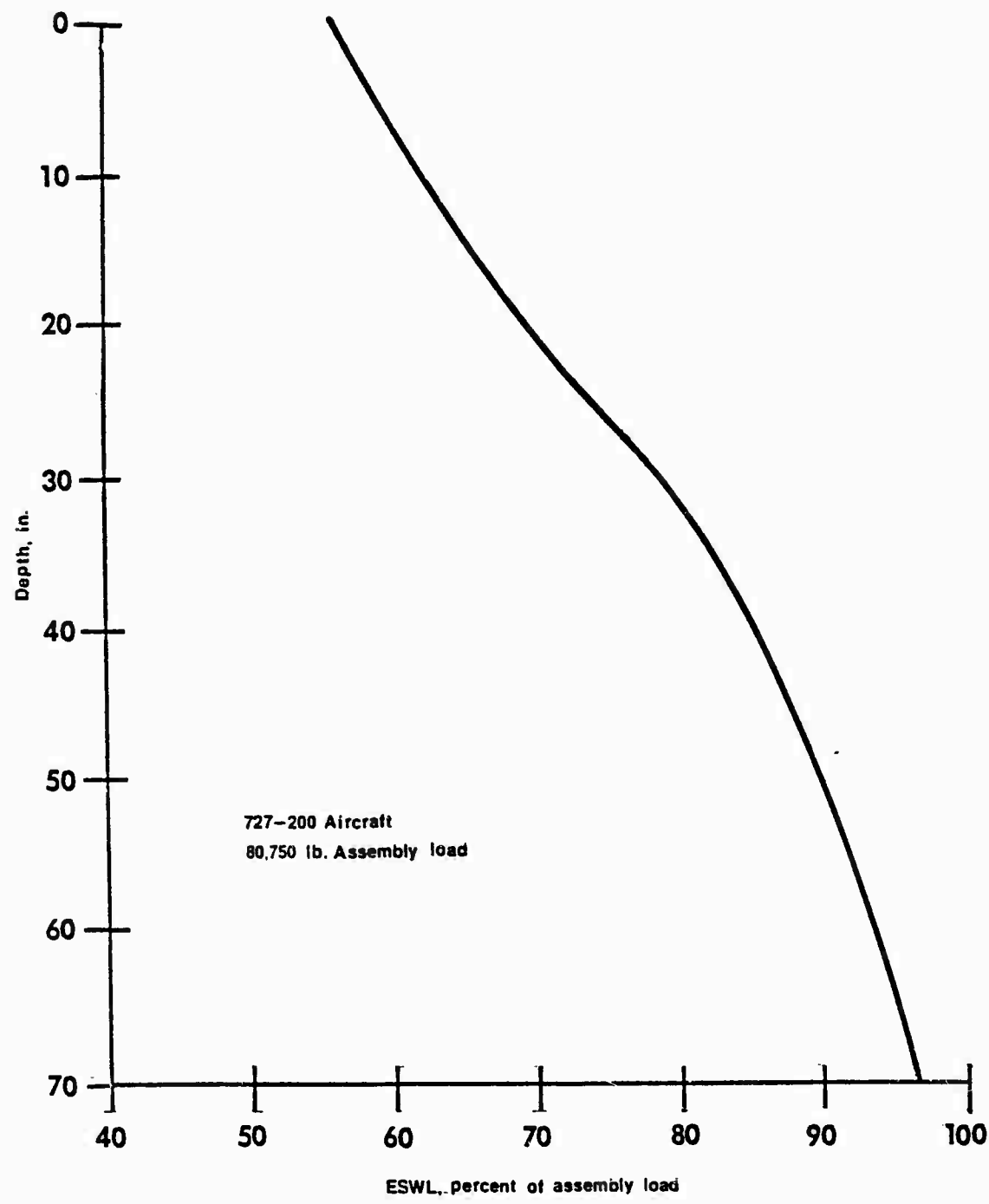


Figure 5-10. ESWL (Percent of Assembly Load) Versus Depth

Table 5-2. CBR Design Curve Development Calculations Summary
727-200 Aircraft, 320,000 Passes

Design Thickness, <i>t</i> (in.)	α_t	Standard Thickness, <i>T</i> (in.)	$\sqrt{A_c}$	$\frac{T}{\sqrt{A_c}}$	$\frac{CBR}{\rho_e}$	ESWL, % of Assembly Load	Assembly Load (lb.)	ESWL(P_e) (lb.)	P_e	CBR
10	0.915	11	15.5	0.71	0.20	62	80,750	50,065	208	41.6
20	0.915	22	15.5	1.42	0.056	68	80,750	54,910	228	12.8
30	0.915	33	15.5	2.13	0.028	78	80,750	63,450	262	7.3
40	0.915	44	15.5	2.84	0.016	84	80,750	67,830	282	4.5
50	0.915	55	15.5	3.55	0.010	88	80,750	71,060	296	3.0
60	0.915	66	15.5	4.26	0.007	93	80,750	75,098	313	2.2
70	0.915	77	15.5	4.93	0.0053	97	80,750	78,328	326	1.7

Table 5-3. CBR Design Curve Development Calculations Summary,
727-200 Aircraft, 64,000 Passes

Design Thickness, <i>t</i> (in.)	α_i	Standard Thickness, <i>T</i> (in.)	$\sqrt{A_c}$	$\frac{T}{\sqrt{A_c}}$	$\frac{CBR}{P_e}$	ESWL. % of Assembly Load	Assembly Load (lb.)	ESWL(P_e) (lb.)	P_e	CBR
10	0.882	11.5	15.5	0.74	0.19	62	80,750	50,065	208	39.5
20	0.882	23.0	15.5	1.48	0.052	68	80,750	54,910	228	11.5
30	0.882	34.0	15.5	2.19	0.025	78	80,750	63,450	262	6.6
40	0.882	45.5	15.5	2.94	0.015	84	80,750	67,830	282	4.2
50	0.882	57.0	15.5	3.68	0.0092	88	80,750	71,060	296	2.7
60	0.882	68.0	15.5	4.39	0.0062	93	80,750	75,098	313	1.9
70	0.882	79.5	15.5	5.13	0.0048	97	80,750	78,328	326	1.6

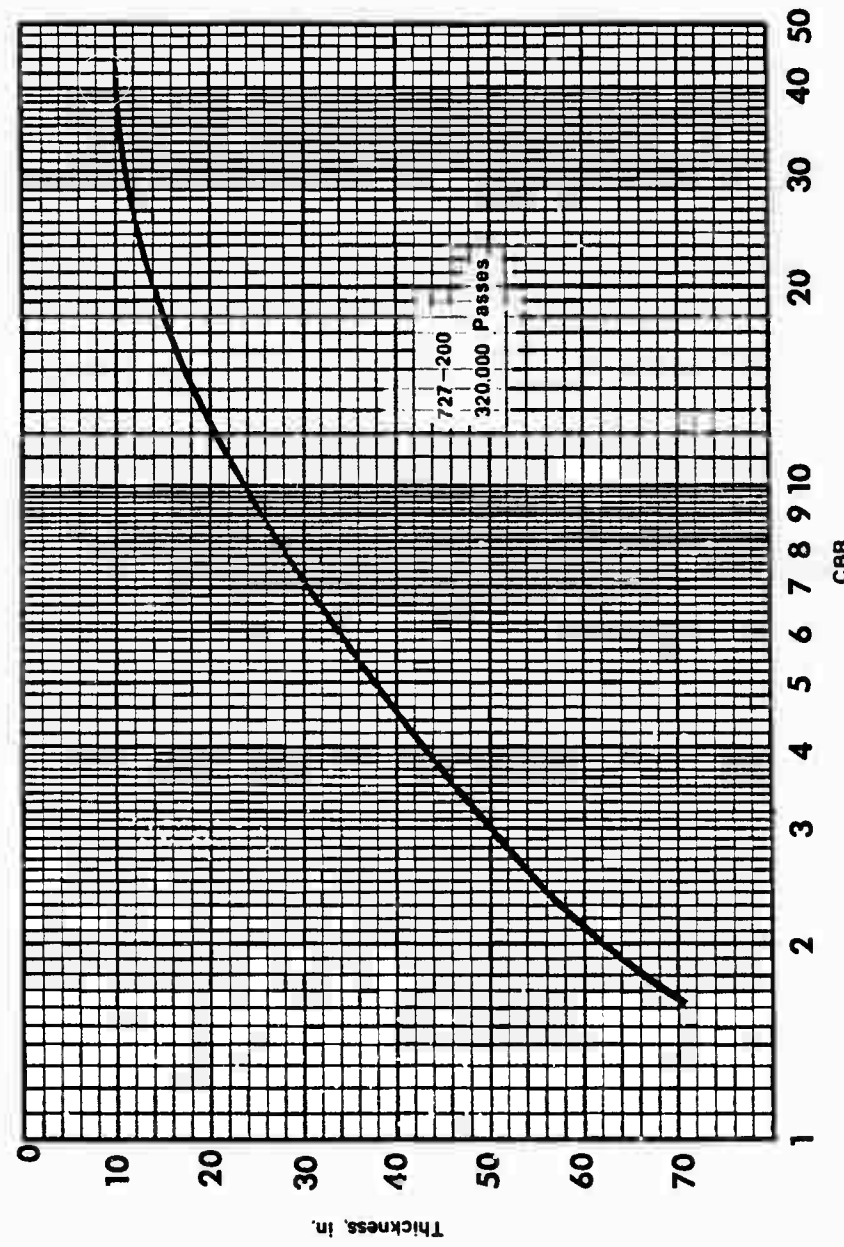


Figure 5-11. Design Curves for Palau Airfield,
727-200 Aircraft, 320,000 Passes

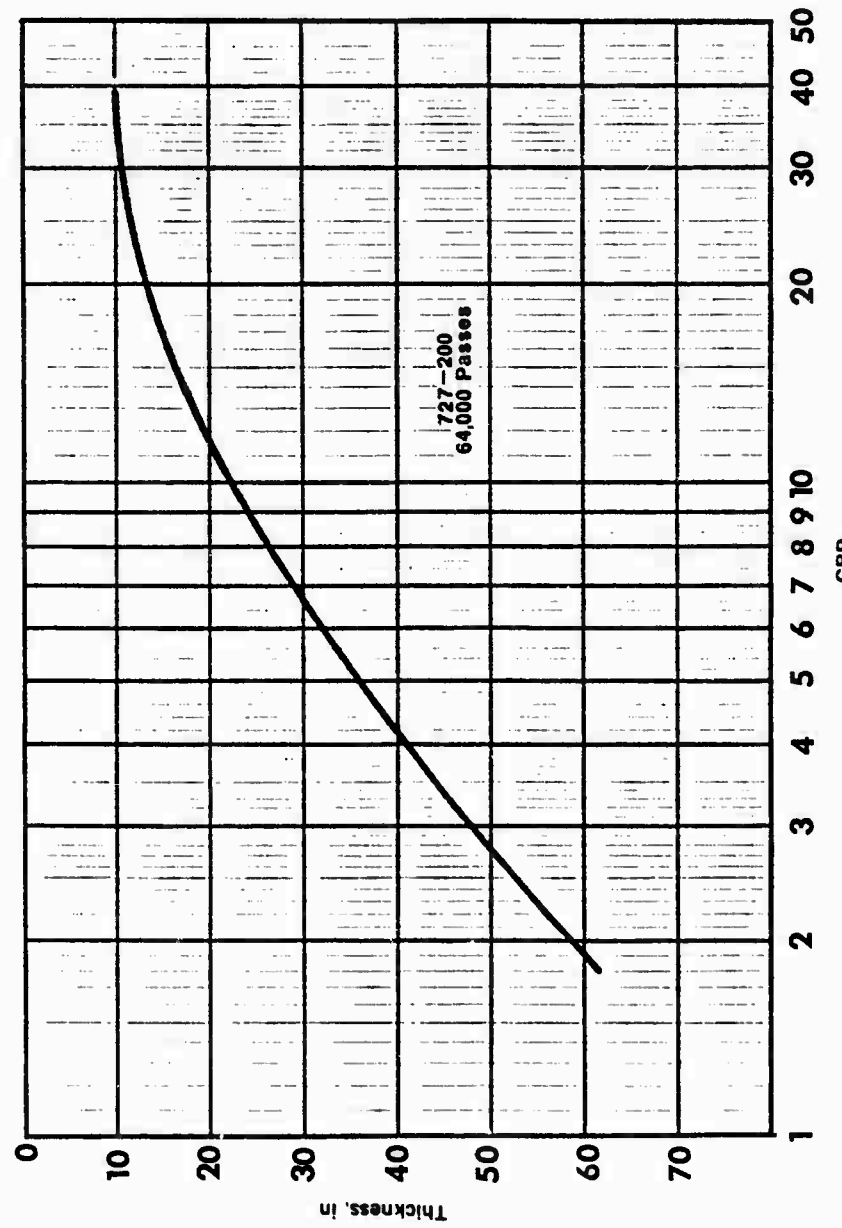


Figure 5-12. Design Curves for Palau Airfield,
727-200 Aircraft, 64,000 Passes

thickness, t , required to protect the subgrade. The same figure is next entered with the subbase CBR of 35 to find a combined base and asphalt layer thickness of 11 inches. This produces a subbase thickness of 38 minus 11, or 27 inches. Using the minimum type "A" traffic, medium load airfield asphalt thickness of 4 inches, a base of 7 inches will be required. This meets the required minimum of 6 inches for a 100 CBR base.

For the type "B" traffic areas, Figure 5-12 is entered with a subgrade CBR of 5. This results in a total thickness of 36 inches. The same figure is next entered with the subbase CBR of 35 and shows a combined base and asphalt thickness of 10 inches. This results in a subbase thickness of 36 minus 10, or 26 inches. Using the minimum type "B" traffic area, medium load airfield asphalt thickness of 3 inches, a base of 7 inches will also be required in these areas. This also meets the required minimum of 6 inches for type "B" areas with a 100 CBR base. Figure 5-13 is a cross-section of the Palau airfield pavement showing the results of the designs just accomplished.

5.4 Comparison of Design Results

Because only one design using the two different methods was compared here, it would be both difficult and unfair to come to any definite conclusions regarding the relative conservatism of the two methods. With regard to the Palau airfield design, the CBR design method has resulted in a similar and slightly less conservative pavement cross-section.

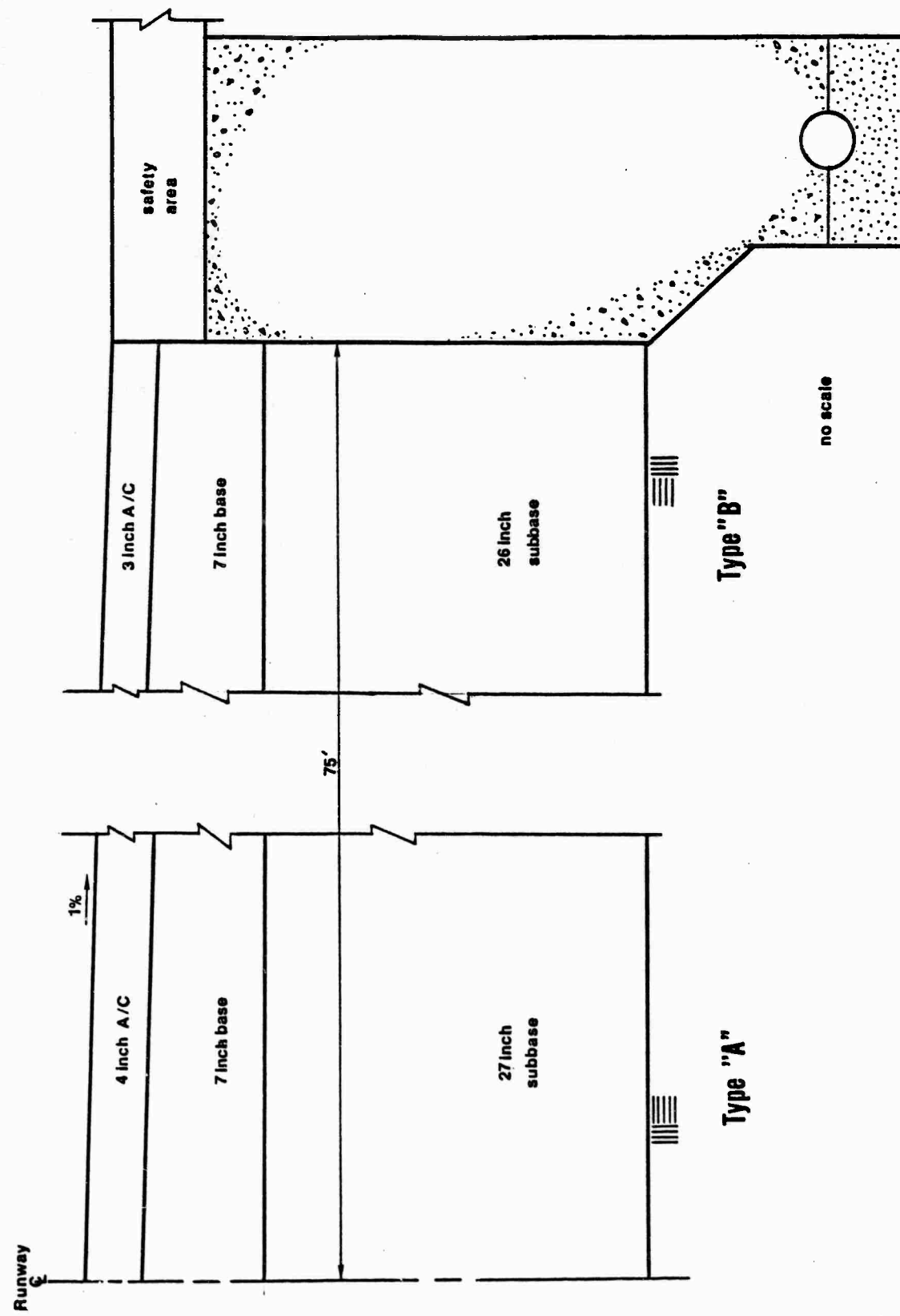


Figure 5-13. Palau Pavement Cross-section, CBR Design

The apparent and relatively conservative nature of the FAA method may be due to the fact that this method is predicated upon a subgrade soil rating system. This rating system ranks soil types based on their FAA soil classification groups, drainage behavior, and frost susceptibility. Therefore, it is possible for major airfield pavements to be designed using the FAA method based solely upon soil classification and the environmental conditions in existence at the site (14:465). It seems logical that such a basis for design, with all of the variables possible within each soil group, would need to be slightly more conservative.

CHAPTER SIX

CONCLUSION

6.1 Conclusion

The intent of this paper has been to present the COE CBR flexible airfield pavement design method and to illustrate its procedure through a case study. This writing has also given a thorough overview of prerequisite topics necessary for an understanding of this and other airfield design methods.

The COE design method was created out of need for a flexible pavement design method dedicated to airfield pavements. It has been the basis for several subsequent flexible design methods. As has been shown, the COE CBR design procedure is clear and concise, and is based on an irrefutable subgrade strength indicator, the CBR index.

In order to simplify the design procedure, computer programs have been developed by the Army that are particularly useful in determining pavement thickness requirements for newly designed aircraft. "Canned" CBR design curves are also available for the various common aircraft in use today, essentially making it necessary only to estimate the number of aircraft loading repetitions and determine the subgrade strength in order to design a flexible airfield pavement.

The author was quite fortunate to have been involved in the construction of the Palau airfield that was presented as a case study in Chapter Five. The airfield was completed in June of 1983 and is

operational today. It offered the U.S. Navy and its associated engineering firms and contractors a real challenge to find ways to utilize high moisture content residual soils for large scale earth fill operations.

The design method just presented is for airfield pavement thickness determination. It should be stressed that very much more goes into the total design of an airfield pavement that was not within the scope of this work. Runway length, alignment, and drainage are a few of the many aspects involved in a total airfield pavement design package.

REFERENCES

1. Ahlvin, R. G., Developments in Flexible Pavement Design in the United States, William Clowes and Sons, Ltd., London, 1971.
2. Brown, Donald N. and George M. Hammit, "Flexible Pavement for Tomorrow's Major Airports," Transportation Engineering Journal, Vol. 95, No. TE 4, November 1969, pp. 617-628.
3. Djou, S. K., Civil Engineer, Hawaii Architects and Engineers, Honolulu, Hawaii, telephone interview, 21 January 1985.
4. Hawaii Architects and Engineers, Inc., Trust Territory Physical Planning Program, Final Report for Palau District, November, 1968.
5. Hawaii Architects and Engineers, Inc., Soils Investigation for Babelthuap-Koror Airport, February, 1978.
6. Horonjeff, R. and Francis X. McKelvey, Planning and Design of Airports, McGraw-Hill Book Company, New York, 1983.
7. Martin, Frederick R. and Raymond F. A. Judge, "Design and Evaluation of Aircraft Pavements," Transportation Engineering Journal, Vol. 99, No. TE 4, November, 1973, pp. 785-799.
8. McCarthy, David F., Essentials of Soil Mechanics and Foundations, Reston Publishing Company, Inc., Reston, 1977.
9. Ralph M. Parsons Company, Environmental Impact Assessment Report, Proposed Babelthuap-Koror Airport, Trust Territory of the Pacific Islands, Palau District, June, 1976.
10. United States Department of the Navy, Airfield Pavements, U.S. Government Printing Office, Washington, D.C., 1973.
11. United States Departments of the Navy, Army, and Air Force, Flexible Pavement Design for Airfields, U.S. Government Printing Office, Washington, D.C., 1978.
12. United States Army Engineers Waterways Experiment Station, Procedures for the Development of CBR Design Curves, U.S. Government Printing Office, Washington, D.C., 1977.
13. Vallerga, Bernard A. and B. F. McCullough, "Pavement Evaluation and Design for Jumbo Jets," Transportation Engineering Journal, Vol. 95, No. TE 4, November 1969, pp. 639-657.
14. Yoder, E. J. and M. W. Witczak, Principles of Pavement Design, John Wiley and Sons, Inc., New York, 1975.